Distribution Agreement

In presenting this thesis as a partial fulfillment of the requirements for an advanced degree from Emory University, I hereby grant to Emory University and its agents the non-exclusive license to archive, make accessible, and display my thesis in whole or in part in all forms of media, now or hereafter known, including display on the world wide web. I understand that I may select some access restrictions as part of the online submission of this thesis. I retain all ownership rights to the copyright of the thesis. I also retain the right to use in future works (such as articles or books) all or part of this thesis.

Signature:

_____ _____

Madison Boswell Date

A Rescue System for GII.4 New Orleans Human Norovirus is Not Dependent on 5' Ribozyme Sequence, Poly-A Tail Length, or Human Codon Optimization

By

Madison Boswell
Bachelor of Science in Biology

Graduate Division of Biological and Biomedical Science
Immunology and Molecular Pathogenesis

_____

Martin Moore, PhD
Adviser

_____

John Altman, PhD
Committee Member

_____

Mandy Ford, PhD
Committee Member

_____

Paul Spearman, MD
Committee Member

_____

John Steel, PhD
Committee Member

Accepted:

_____

Lisa A. Tedesco, Ph.D.
Dean of the James T. Laney School of Graduate Studies

_____

Date

A Rescue System for GII.4 New Orleans Human Norovirus is Not Dependent on 5' Ribozyme Sequence, Poly-A Tail Length, or Human Codon Optimization

by

Madison Boswell
Bachelor of Science in Biology

Thesis Adviser:

Martin Moore, PhD

Thesis Committee:

John Altman, PhD
Mandy Ford, PhD
Paul Spearman, MD
John Steel, PhD

An abstract of
A thesis submitted to the faculty of the
James T. Laney School of Graduate Studies of Emory University
in partial fulfillment of the requirements for the degree of
Master of Science
in Immunology
2015

Abstract

A Rescue System for GII.4 New Orleans Human Norovirus is Not Dependent on 5' Ribozyme Sequence, Poly-A Tail Length, or Human Codon Optimization
by Madison Boswell

Human Norovirus is a serious health problem that is understudied due to a lack of tractable rescue systems for understanding virus biology. Since its discovery nearly half a century ago, Norovirus has proven a difficult virus to study because pure virus alone does not replicate in any known cell culture system, there is no physiological small animal model, and there exists only inefficient rescue systems for the virus. The lack of a model system in which to study the virus has lead to a paucity of understanding of even basic features of the virus life cycle, general biology, and pathogenesis in humans. The goal of this research endeavor was to adapt the published rescue systems for Norovirus to the clinically relevant GII.4 New Orleans genotype, to increase precision of viral transcripts through the use of ribozymes, and to increase protein expression through human codon optimization, all with the aim of increasing the likelihood of successful recovery of infectious human Norovirus.

A cDNA clone encoding a full-length genome for GII.4 human Norovirus was cloned under control of a T7 promoter sequence. This clone featured a number of modifications upon the published rescue systems for GII.3 Norovirus, including a 5' ribozyme sequence between the T7 promoter and the 5' UTR of the Norovirus genome, as well as a longer poly-A tail corresponding to the natural poly-A tail of human Norovirus (HuNoV). In addition to this base genome, another construct was assembled featuring GII.4 HuNoV cDNA optimized for protein expression in human cells. This optimization relies on a concept known as codon bias, or the genomic frequency of certain codons for a given amino acid. All reading frames of the HuNoV genome in this construct were modified to match human codon bias to increase viral protein expression in an attempt to improve viral rescue efficiency in mammalian cells.

These modifications did not result in measurable protein expression, and neither RNA replication nor viral protein expression was detected in cells transfected with either construct. This thesis demonstrates that GII.4 Norovirus rescue is not dependent on codon optimization, 5' ribozyme sequence, or poly-A tail length.

A Rescue System for GII.4 New Orleans Human Norovirus is Not Dependent on 5' Ribozyme Sequence, Poly-A Tail Length, or Human Codon Optimization

by

Madison Boswell
Bachelor of Science in Biology, Davidson College, 2009

Thesis Adviser:

Martin Moore, PhD

Thesis Committee:

John Altman, PhD
Mandy Ford, PhD
Paul Spearman, MD
John Steel, PhD

A thesis submitted to the faculty of the
James T. Laney School of Graduate Studies of Emory University
in partial fulfillment of the requirements for the degree of
Master of Science
in Immunology
2015

Acknowledgements

First and foremost I would like to thank my wife Katie for your incredible kindness and support every step of the way through this graduate process; I could not have made it this far without you. Thank you to my parents and family for your support both before and during graduate school. Thank you to my friends who helped me through difficult times and reminded me that there is much that is good in life. Thank you to my labmates for aiding me while I chased down multiple avenues of scientific query and putting up with endless questions and thought experiments.

Thank you to my adviser, Dr. Marty Moore, for your support and advice in tackling this project. Thank you to my committee members for agreeing to serve on my committee and for helping me to establish a solid foundation for this thesis. Thank you to everyone, friends, family, and others who took the time to help me proofread and assemble this thesis; I appreciate all of your tireless work. Thank you also to my former mentors and labmates, who have helped me from afar with kindness and support.

Finally, I would like to thank Dr. Moe and Dr. Kirby for their help in getting started with a new virus for our lab. I very much appreciate all of your help and the generous gifts of antibodies and reagents.

Table of Contents

Chapter 1
Introduction – An Overview of Human Norovirus

Discovery

In 1929, pediatrician Dr. John Zahorsky was the first to describe Norovirus-induced gastroenteritis in infants, labeling it “Hyperemesis hiemis or winter vomiting disease” [1]. This initial characterization of viral gastroenteritis did not describe a causative agent, which went undiscovered until Dr. Albert Kapikian and colleagues positively identified the Norovirus prototype Norwalk Virus in 1972 [2]. Prior to 1972, scientists had unsuccessfully attempted to identify the etiologic agent of nonbacterial acute gastroenteritis through studies involving transmission of stool samples between volunteers, despite significant interest throughout the 1940s and 1950s and again in the early 1970s. A study by Dolin et al. from 1971 describes the serial passage of a filtered rectal swab specimen from an infected adult into volunteers a total of three times [3]. Characterization of the challenge patients’ stool samples indicated that the infectious agent was less than 66nm in diameter and that it was not inactivated by ether, acid, or heating at 60°C for 30 min, suggesting a viral causative agent [2, 3].

The following year, Kapikian et al. adapted the technique of immune electron microscopy, previously used to detect rubella virus, to search for infectious particles in preserved stool samples isolated from an outbreak of gastroenteritis at Bronson Elementary School in Norwalk, Ohio four years prior [2]. In this study, cryopreserved inoculum from the 1968 Norwalk outbreak was administered orally to a volunteer, and the filtered stool of that volunteer was passaged into a second volunteer [2]. The stool of this second patient, who developed acute gastrointestinal illness akin to the original outbreak, was sequentially filtered through 1,200 nm and 450 nm membrane filters and diluted 1:50 in veal infusion broth containing 0.5% bovine serum albumin, resulting in a 2% filtrate. This filtrate was examined utilizing inactivated convalescent serum from other experimentally infected volunteers in the hopes of aggregating the virus, thereby facilitating visualization by electron microscopy [2]. The serum-stool filtrate mixtures were incubated for one hour at room temperature and centrifuged to collect the pelleted sediment, which was resuspended with distilled water, stained with 3% phosphotungstic acid, placed onto a formvar/carbon-coated grid, and examined at 40,000 times magnification via electron microscopy [2]. The authors observed large aggregates of small, rounded viral particles resembling picornavirus or parvovirus that stood out clearly from the surrounding matter and appeared to exhibit cubic symmetry [2]. No further structural characterization could be determined from these aggregates. These aggregates were observed at a higher frequency when mixed with post-challenge serum of infected individuals, indicating that the viral infection induced an antibody response specific to these observed aggregate particles [2]. In one challenge volunteer who did not develop illness, no increase in the number of viral aggregates was observed, suggesting a causative relationship between the aggregate viral particles and development of acute gastrointestinal symptoms [2]. Additionally, Kapikian et al. subjected their volunteers to heterologous challenge with filtered stool samples from outbreaks in Hawaii and Maryland in conjunction with stool samples from the Norwalk outbreak to determine specificity of the immune response to the virus. The Maryland sample induced seropositivity to the Norwalk virus in one volunteer, though the serum

response was insufficient to prevent infection upon Norwalk challenge [2]. Furthermore, aggregation of the Maryland agent increased following challenge with the Norwalk agent, suggesting an incomplete initial immune response to the Maryland virus [2]. The Hawaii challenge strain did not induce heterotypic immunity, and had no effect on the serum against the Norwalk strain [2]. Kapikian also noted that of the 13 individuals tested, including those who did not develop symptoms, each individual had antibody in the pre-challenge, acute-phase, or early post-challenge sera, suggesting that baseline immunity to this virus may be widespread among the population [2].

Etymology

The term Norovirus refers to a genus of virus, rather than a species of virus. The genus Norovirus comprises only a single species, Norwalk virus, named in honor of the town Norwalk, OH, whence originated the first isolate identified in 1972 by Kapikian and colleagues [2]. The International Committee on Taxonomy of Viruses originally assigned this prototypic Norwalk virus to the *Caliciviridae* family and the now defunct *Calicivirus* genus in 1995 [4]. Members of the family *Caliciviridae* are nonenveloped, small, single-stranded, nonsegmented, positive sense RNA viruses, named for the cup- or chalice-(Latin *calyx)* shaped depressions on the surface of the virion visible by electron microscopy [5]. In 1998, the ICTV created a new genus named "*Norwalk-like viruses*" to separate Norwalk viruses from the other members of the *Caliciviridae* family: the Vesiviruses, including Swine vesicular exanthema virus, the Lagoviruses, which contain Rabbit hemorrhagic disease virus, and the Sapporo-like viruses, which contain the Sapporo virus, another cause of gastroenteritis in humans [6]. In 2002, this "*Norwalk-like viruses*" genus was renamed "*Norovirus*," again in honor of Norwalk, OH [6]. The *Caliciviridae* family has not been assigned an order designation from the ICTV, and the *Norovirus* genus similarly has not been assigned a subfamily under *Caliciviridae* [6].

To distinguish various outbreaks, Noroviruses are categorized based on sequence analysis of the major component of the capsid shell VP1. This approach has become the dominant tactic for categorizing Norovirus since the early 2000s; prior to that point, cross-challenge studies in volunteers and cross-reactivity analyses by immune electron microscopy had been used with limited success [7, 8]. These early approaches were plagued by poor reproducibility, as antibodies to Norovirus were inconsistently cross-reactive. Furthermore, neutralization assays were impossible due to the inability to culture the virus *in vitro*. Jiang et al. began using reverse transcriptase polymerase chain reaction (RT-PCR) to analyze the virus and detect differences in the second reading frame, which encodes VP1 [8]. ORF2 sequence differences detected by RT-PCR revealed five unique genogroups of Norovirus, termed GI, GII, GIII, GIV, and GV; each genogroup featured 45-61% uncorrected pairwise difference in the VP1 region sequence [8]. GI and GII viruses are responsible for the majority of human Norovirus infections, while GIII viruses infect cattle, GIV viruses commonly infect dogs and rarely infect humans, and GV viruses infect mice [8]. These genogroups were further divided by their predicted 3D structure as determined by Zheng et al. in 2006, wherein the authors performed a Bayesian analysis of the VP1 homology to split the Norovirus genogroups into genetic clusters, or genotypes [7]. GI Norovirus was split into 8 genotypes, GII into 17 genotypes, and GIII into 2 genotypes, while GIV and GV

Norovirus were each assigned only a single genotype [7]. Even within these genotypes, such as GI.1 (the prototypic Norwalk virus) or GII.4 (the current prevailing strain worldwide), different Norovirus outbreaks are further identified by the city in which the outbreak was first detected, for example GI.4 Chiba named for an outbreak in 2000 in Chiba, Japan or GII.4 Sydney, named for an outbreak in Sydney, Australia in 2012 [9, 10]. These outbreaks may spread from the initial location yet retain their original name, as is the case for the GII.4 Sydney virus, which is currently the prevailing cause of Norovirus outbreaks in the United States [10].

Controversy has arisen over improper use of the term *Norovirus*, which refers to the genus of virus, and not individual species or outbreaks. This controversy originates from the original designation of the causative agent of the Norwalk outbreak: genus *Norwalk-like viruses*, species *Norwalk virus* [4]. The genus *Norwalk-like virus* was later renamed *Norovirus*, while the species retained its name of *Norwalk virus* [6]. This fact, coupled with the fact that Norwalk viruses are often named for other cities undergoing outbreaks, generates confusion over the proper nomenclature. The ICTV recommends the use of the term Norwalk virus when referring to individual outbreaks [6]. The media and many health officials however, including the Centers for Disease Control and Protection, utilize the term Norovirus to refer to any outbreak caused by a member of the *Norovirus* genus [11]. Further controversy has arisen among Japanese scientists due to Noro being a common Japanese surname. These scientists support the use of the “Norwalk Virus” species name rather than the “Norovirus” genus name to refer to outbreaks in order to reduce social stigma associated with the virus.

Other common or incorrect names for Norovirus include food poisoning, which is not limited to Norovirus infections, the winter vomiting bug, as Norovirus is known in the United Kingdoms, or the stomach flu, a misnomer which is colloquially used to refer to acute viral gastroenteritis despite the fact that Norovirus is not at all associated with influenza [11].

Genome

Human Norovirus (HuNoV), like all members of the *Caliciviridae* family, is encoded by a relatively short, single-stranded, nonsegmented positive-sense RNA genome. The genome ranges in length from 7.3 to 7.5 kilobases (kb), varying by strain, and comprises 3 conserved open reading frames (ORFs) [12]. The genomic RNA is not capped, but is instead conjugated at the 5’ end to the viral protein VPg, short for viral protein, genome-linked [12]. Following the VPg cap is a short untranslated region (UTR) at the 5’ end of the genome, which ranges from 3 nucleotides (nt) in many HuNoV isolates to 5 nt in a murine Norovirus (MNV)-1 isolate [13]. These UTRs feature secondary structures important for viral protein translation [14-16]. The first open reading frame, ORF1, encodes a large polyprotein containing at least six mature non-structural (NS) protein products [12]. These NS proteins are cleaved during and post-translation from the polyprotein by the viral protease, itself a catalytically active component of the polyprotein [17]. ORF1 overlaps ORF2 by around 20nt. ORF2 encodes the major capsid protein VP1 in an alternate reading frame from ORF1 [12]. ORF2 is not co-translated with ORF1, and is instead translated from a VPg-capped,

polyadenylated subgenomic RNA produced during viral replication [12]. ORF3, which encodes the minor capsid protein VP2, overlaps with the 3' end of ORF2 by as little as a single nucleotide in some sequences [12]. ORF3 encodes protein in a reading frame separate from ORF2 [12]. ORF3 is followed by a 3' UTR, which also forms secondary structures important in initiation of viral protein translation [14-16]. Finally, the genome is polyadenylated at the 3' end with 34-150 adenosine residues [18, 19].

The first protein translated following infection of a cell is the ORF1-encoded viral polyprotein comprising at least 6 individual protein subunits [17]. The 5'-most protein is the nonstructural protein p48, also called N-terminal nonstructural protein, an approximately 398 amino acid protein of calculated mass 45kDa that varies in length and sequence between Norovirus genogroups [20]. This protein shows no broad sequence or structural homology to any other viral or cellular proteins and its function is not currently understood. Hughes et al. identified H box/NC motifs in p48 that may play a role in the regulation of cell cycle [17, 21]. Ettayebi et al. demonstrated that p48 forms a complex with the SNARE regulator VAP-A by yeast two-hybrid screen, suggesting that p48 may play a role in cellular protein trafficking, as surface expression of vesicular stomatitis virus G glycoprotein was inhibited when cells were co-transfected with HuNoV p48 [22]. A hydrophobic domain of p48 predicted by sequence analysis may play a role in anchoring the replication complex to intracellular membranes, where replication of RNA viruses occurs [17]. Norovirus p48 has been compared to Hepatitis C virus NS5A protein, which serves as a scaffolding protein and also interacts with VAP-A [17]. Finally, transfection of CRFK cells, a feline kidney cortex cell line, or HeLa cells, a human cervical carcinoma cell line, with an expression vector encoding HuNoV p48 caused disruption of the Golgi apparatus, though the authors state this disassembly may be due to simple overexpression of p48 and may not reflect a physiological function of the protein [20].

The second protein constituent of the HuNoV viral polyprotein is the nucleoside triphosphatase (NTPase) p41, a member of the RNA helicase superfamily 3 [23]. This protein shares sequence motifs with picornavirus protein 2C, and binds and hydrolyzes ATP *in vitro* [23]. Like picornavirus 2C, p41 lacks helicase activity, but unlike 2C p41 is capable of hydrolyzing all NTPs rather than only ATP. ATP binding activity is lost following mutation of amino acid 168 of the protein [23]. Furthermore, ATPase activity of p41 is not hindered by the denaturant guanidium chloride, unlike picornavirus 2C [23].

The third protein component of the polyprotein is the p22, or 3A-like protein, so named for its similar position within the genome to 3A protein of picornavirus. p22 shares minimal sequence homology compared to 3A or homologs in other caliciviruses. Like p48, the function of p22 has not yet been elucidated, though p22 also shares a putative hydrophobic region in the central domain [17]. This region may facilitate trafficking to internal membranes, a hypothesis consistent with the finding that in feline calicivirus the p22 homolog plays a role in the assembly of membrane complexes for viral replication [24].

The fourth protein encoded by ORF1 is the RNA capping protein known as “viral protein, genome-linked” or VPg. VPg is a 15kDa protein covalently linked to the 5’ end of genomic and subgenomic RNA in animal caliciviruses, and many hypothesize that it functions similarly in HuNoV infections [17]. VPg recruits ribosomes to the viral RNA by interacting directly and specifically with eukaryotic initiation factor 3 (eIF3) and 40S ribosomal subunits [25]. In the absence of VPg conjugation, RNA genomes are not efficiently translated and are generally noninfectious. Sosnovtsev et al. published in 1995, however, that RNA transcripts derived from a full-length clone of the FCV Urbana genome are infectious and are translated in the absence of VPg, though a traditional methyl-7-G cap was required in place of VPg [26]. This finding was expanded by Herbert et al. who demonstrated that removing VPg of FCV via proteinase K treatment resulted in no change in the site of RNA initiation, but a significant decrease in RNA translation [27]. Furthermore, translation of FCV viral proteins was dependent on VPg binding directly to eIF4E in an *in vitro* rabbit reticulocyte translation assay [28]. The selective eIF4E inhibitor 4E-BP1 reduced translation of VPg-conjugated RNA compared to RNA featuring an internal ribosomal entry sequence (IRES) from encephalomyocarditis virus (EMCV), but 4E-BP1 did not interfere with binding of VPg to eIF4E [28]. In MNV-1, the C-terminal domain of VPg directly binds the eIF4F complex via high affinity interactions with eIF4G and eIF4E, though depletion of eIF4E did not alter MNV-1 translation [29, 30]. The VPg of rabbit hemorrhagic disease virus (RHDV), a lagovirus and member of the *Caliciviridae* family, is uridylylated at tyrosine 21 by the RNA-dependent RNA polymerase as a precursor to RNA extension [31]. Human Norovirus is nucleotidylylated in similar fashion by the ProPol polyprotein product at Tyrosine 27 rather than Tyrosine 21 [32]. The mechanism of VPg priming of RNA replication may differ between HuNoV VPg and picornavirus VPg based upon the varying molecular weights of the two molecules (15kDa vs. 2-4kDa) [17].

The fifth protein constituent of the HuNoV polyprotein is the 3C-like protease or Pro, named for its functional and positional similarity to the picornavirus 3C protease [17]. This protein is catalytically active following translation while still part of the viral polyprotein.[17] HuNoV pro cleaves at various positions within the polyprotein with different substrate specificities. Liu et al. demonstrated that QG dipeptides, similar to the preferred recognition sites for the picornavirus protease, located at glutamines 399 and 762 in a rabbit reticulocyte model of translation, were the targets of Southampton Virus protease [33]. Q to P site-directed mutagenesis of these residues completely abolished cleavage of the polyprotein and subsequent release of p41, identified in the 1996 report as the 2C-like helicase [33]. In a follow-up report, the same research group identified additional substrates for Southampton Virus protease at the EG dipeptides located at the N termini of VPg (aa 961) and Pol (aa 1280), as well as the EA dipeptide located at residue 1099 between VPg and Pro in an *E. coli* expression system [34]. These five restriction sites permit complete cleavage of the viral polyprotein into the six protein products without additional cleavage by cellular proteases.

The sixth and largest protein component of the polyprotein is the 58kDa RNA-dependent RNA polymerase (RdRP), or Pol [35]. The first calicivirus RdRP to be identified was RHDV Pol, first identified in 1998 by Vazquez and colleagues following

expression in *E. coli* utilizing a glutathione *S*-transferase-based vector [35]. RdRP activity was measured at 30°C for one hour with a radiolabeled UTP using synthetic RHDV subgenomic RNA lacking VPg and with an A_{18} tail as a template. RNA was then electrophoresed in a formaldehyde-agarose gel and radiolabeled RNA was detected by autoradiography, where the synthesis of novel RNA of appropriate length was detected in an RNAse A-sensitive manner [35]. The crystal structure of RHDV RdRP was determined in 2001; like the polymerases of other ssRNA viruses, RHDV Pol features elements resembling a “right hand,” including the fingers, palm, and thumb domains [36]. This study methodology was carried over to a Spanish isolate of Norwalk virus Ast6139/01/Sp in 2004, which was found to have an RdRP similar to that of RHDV. Unlike RHDV RdRP, however, Norwalk virus RdRP featured a carboxy-terminal segment located in the active site cleft of the protein when expressed in *E. coli* [37]. This carboxy-terminal domain exhibited homology to the Beta-loop insertion in the thumb domain of Hepatitis C Virus (HCV) RdRP, a domain which potentially stabilizes primers during RNA synthesis initiation [17].

ORF2 of the Norovirus genome encodes the major capsid structural protein VP1. This 530-555 amino acid, 58-60kDa protein is translated not from full-length genomic RNA, but rather from a VPg-conjugated subgenomic RNA generated during the virus life cycle [19]. The VP1 monomer structure has been determined by X-ray crystallography at 3.4-Angstrom resolution following overlay on a 22-Angstrom cryo-electron microscopy model [38]. Each monomer features 3 domains: the N-terminal or N domain, comprising amino acids 10-49 which face the interior of the assembled virion, the Shell or S domain, comprising amino acids 50-225 which play an important role in the icosahedral assembly of the virion, and the protruding or P domain, comprising amino acids 226-520 which are involved in virion stability and which form the external surface of the virion [38]. The P domain is further divided into three subdomains, including two P1 subdomains spanning amino acids 226-278 and 406-520, which play a role in dimerization of the major capsid protein, as well as the P2 subdomain, a segment spanning amino acids 279-405 that forms the majority of external structures of the virion. P2 features a hypervariable region which, when mutated, alters immunogenicity and substrate binding of the virion [39]. Tan et al. also hypothesize that the hypervariable portion of the P2 domain is necessary for HBGA interaction, and thus species specificity of HuNoV [39].

VP1 is the primary constituent of the virus capsid, which self-assembles from 90 dimers of VP1 and 1-2 copies of the minor capsid protein [40]. This self-assembly was first described by Jiang et al. who observed complete viral capsid assembly when VP1 was exogenously expressed in a cell-free translation system using recombinant baculovirus [41]. This same capsid was also detected by purification of 58kDa protein from *Spodoptera frugiperda 9* (Sf9) cells transfected with recombinant subgenomic RNA, followed by N-terminal amino acid sequencing [41]. Furthermore, these self-assembling particles induced antibody responses in experimentally treated mice and bound to anti-HuNoV antibodies in the serum of volunteers [41]. These findings formed the basis for the design of a VLP-based vaccine approach to Norovirus, which has seen modest success in clinical trials [42].

ORF3 of the genome encodes the structural protein VP2, or the minor capsid protein. This protein varies in sequence and length from 208-268 amino acids based on strain, correlating with a molecular weight of 22-29kDa. VP2 is translated from the VPg-conjugated subgenomic RNA via an alternate reading frame, and the protein is present as a minor proportion in the virion, with only 1-2 proteins per assembled virus particle in the RHDV model of HuNoV, FCV, and Norwalk Virus [43-45]. Glass et al. determined that VP2 is basic with an isoelectric point of 10.99, and hypothesized that it may aid in binding acidic RNA, as the inner faces of capsids derived exclusively from VP1 are acidic and thus not amenable to RNA binding [45]. Further circumstantial evidence supporting this hypothesis exists in the fact that VP1 of HuNoV lacks the N-terminal RNA-binding domain observed in other viruses featuring a single-protein capsid, namely tomato bushy stunt virus [46]. Sosnovstev et al. published in 2005 that VP2 is essential for the production of infectious virions in the FCV model [47]. When capped genomic RNA or plasmid DNA of mutants with an early stop codon in VP2 were transfected into CRFK cells, no development of cytopathic effects (CPE) was observed [47]. The general cell morphology and intracellular distribution of expressed VP1 as measured by immunofluorescent staining indicated that virus replication and translation had occurred, but no capsids could assemble in the absence of VP2 [47]. There is not yet direct experimental evidence demonstrating that VP2 directly binds RNA, but Hardy hypothesizes that VP2 may bind to VPg instead of RNA directly, thus facilitating genome incorporation into the nascent capsid [17].

Life Cycle

The human Norovirus life cycle begins when the virus binds to its receptors and enters the cell. HuNoV interacts with the numerous and varied human histo-blood group antigens (HBGAs) to aid in infection as demonstrated by Jones et al. [48]. In a model of HuNoV infection of B cells, addition of synthetic HBGA or enteric bacteria displaying HBGA on their surface increased Norovirus infectivity of B cells in a dose-dependent manner [48]. The protruding P domains of the capsid have been co-crystallized with a panel of HBGA types and show both remarkable specificity and marked evolution over the course of the most recent Norovirus epidemics [49]. Little is known specifically about HuNoV following attachment to target cells because until recently no cell model has been available to dissect life cycle steps; to circumvent this deficiency, many other calicivirus models for HuNoV have been studied to identify commonalities between viruses likely to extend to HuNoV.

In contrast to the HBGA affinity of HuNoV, feline calicivirus (FCV) utilizes junctional adhesion molecule 1 (JAM-1) as its functional receptor, highlighting the likelihood that other caliciviruses may not serve as an exact model for HuNoV biology [50]. Upon binding its JAM-1 receptor, FCV capsid undergoes significant structural changes focused at the interface of the protruding P domain of the major capsid protein, which may play a role in entry [51]. Additional requirements for clathrin-mediated endocytosis as well as endosomal acidification have been demonstrated for FCV [52]. When endosomal acidification is blocked using chloroquine and bafilomycin A1 in Crandell-Reese feline kidney (CRFK) cells, FCV fails to permeabilize the membrane,

and uncoating of the genome is stopped [52, 53]. This effect of chloroquine is reversible, and once the drug is removed FCV infection proceeds normally [53]. In porcine enteric calicivirus, bile acids may play a role in acidification and thus activation of the viral capsid within 1-4 hours following infection, though the precise mechanism has yet to be described [54]. Endosomal cathepsin L may also play a role in capsid disassembly; recombinant cathepsin L cleaves VP2 of porcine enteric calicivirus (PEC) or VP1 of MNV and FCV as measured by western blot [55]. When cells infected with FCV were treated with cathepsin L inhibitor or with chloroquine, intact virus capsids were retained in the endosomes, and infectivity was decreased [55].

In the MNV model of HuNoV infection, the ganglioside-linked terminal sialic acid moieties GD1a, GM1, and asioalo-GM1 (GA1) on mouse macrophages serve as the attachment receptors, rather than the HBGAs [56]. When these gangliosides were depleted using the glycosylceramide synthase inhibitor d-threo-P4, MNV-1 binding to both cultured and primary mouse macrophages was decreased, resulting in approximately 40-80% less infection as measured by plaque assay [56]. This loss of infectivity was rescued through the addition of free ganglioside GD1a or GA1 [56]. Once bound by its ganglioside receptors, MNV-1 enters mouse macrophages by an unidentified pathway. This method of entry into the RAW264.7 murine macrophage cell line is not dependent on clathrin or caveolin, but does rely on dynamin and cholesterol pathways [57]. RAW264.7 cells do not express caveolin, and interfering with the clathrin pathway through the dominant negative Eps15 or adaptin-2 complex did not diminish MNV-1 infectivity [57]. Flotillin depletion and endosomal acidification blockers also did not reduce infectivity, in contrast to the effects observed in the closely related calicivirus FCV [57]. Methyl-beta-cyclodextrin and dynasore, a dynamin inhibitor, reduced MNV-1 infectivity only when cells were treated before and not after infection, implicating cholesterol and dynamin pathways in viral entry without describing a specific mechanism [57]. Macropinocytosis in infected RAW264.7 cells was disrupted through the addition of 5-(N-ethyl-N-isopropyl) amiloride or through actin disruption, but these processes enhanced rather than disrupted virus infectivity, suggesting that methods of endocytosis other than macropinocytosis are candidates for MNV-1 entry [57].

Once the VPg-conjugated genomic RNA has reached the cytoplasm of the host cell, the viral polyprotein is translated by host machinery following recruitment of ribosomes to the VPg in an initial round of viral RNA translation dubbed “pioneer” translation [12, 25]. Viral polyprotein is translated and autocatalytically cleaved by its protease component in two distinct cleavage steps: “early” and “late” cleavage. Early cleavage occurs between the QG dipeptides to release the 5’ p48 N-terminal and p41 NTPase proteins. Late cleavage may follow one of two predicted pathways. The first pathway involves cleavage at the EA dipeptide between VPg and Pro, releasing a p22VPg product and a ProPol product, which appears to have enzymatic functionality as a uridylylator of VPg [32, 58]. The second and more complete cleavage pattern involves cleavage at the EG dipeptide downstream of Pro to release Pol, followed by subsequent cleavage at the EG dipeptide downstream of p22 to release p22. The final cleavage then occurs at the EA dipeptide between VPg and Pro to release all 6

individual proteins from the viral polyprotein [58]. These cleavage products were detected *in vitro* and *in vivo* in various animal calicivirus models [58].

Once the 6 nonstructural proteins have been liberated, the viral polymerase forms a replication complex in association with host membrane complexes in the cytoplasm, or in association with the endoplasmic reticulum and endosomes [59, 60]. This replication complex may include other nonstructural proteins, but direct evidence for HuNoV replication complex formation is lacking due to the unavailability of a culture model with robust replication. During infection with MNV-1, genome replication as measured by double-stranded (ds)-RNA occurs at punctate foci surrounding the nucleus [12]. The replication complex binds template RNA to initiate replication, which occurs in two steps. The first step is synthesis of negative sense antigenomic RNA using the VPg-conjugated genomic RNA as a template for *de novo* RNA synthesis, a process that does not appear to require VPg conjugated to the template strand [18]. Furthermore, it is unclear if the nascent antigenomic RNA strand is VPg conjugated as well; Subba-Reddy et al. hypothesized in 2012 that *de novo* and thus VPg-independent synthesis of RNA is the primary source of negative-sense and subgenomic RNA [61]. This synthesis is dependent on interactions with the VP1 major capsid protein in a cell-based assay utilizing a luciferase reporter downstream of RIG-I sensing of 5' triphosphorylated RNA [61]. The second step of replication is the synthesis of positive sense genomic and subgenomic RNAs using the antigenomic RNA as a template; this process is thought to be VPg-dependent in HuNoV [62]. Subgenomic RNAs, like genomic RNAs, are positive sense and VPg conjugated, though the two overlap by a number of nucleotides and encode protein in separate reading frames. Synthesis of subgenomic RNA occurs by one of two hypothesized routes: early termination of antigenomic RNA replication, which produces a truncated antigenomic RNA copy that serves as a template for subgenomic RNA synthesis, or initiation of RNA replication at a secondary structure upstream of ORF2 in the negative-sense antigenomic RNA [12]. This second model is supported by the presence of a conserved RNA stem-loop structure 6nt from the start of the subgenomic RNA [16]. Translation from the newly replicated genomic RNA gives rise to additional virus polyprotein, while translation of exclusively subgenomic RNA is responsible for ORFs 2 and 3 expression of VP1 and VP2 [12]. Translated VP1 and VP2 assemble into virions, which encapsidate the VPg-conjugated genomic RNA. The assembled virus is released from the cell by an unknown mechanism. Alonso et al. demonstrated that assembled RHDV virions are released from host cells through the induction of apoptosis [63]. Bok et al. demonstrated that a similar release mechanism is employed by MNV, which downregulates host cell survivin in order to induce apoptosis [64]. Further studies using a tractable cell culture method for HuNoV are necessary to understand this final step in the virus life cycle.

Epochal Evolution

Emerging strains of GII.4 human Norovirus have been recently associated with at least eight epidemic seasons in the winters of pre-1995 (Camberwell), 1995-1996 (Grimsby), 2002-2003 (Farmington Hills), 2004-2005 (Hunter), 2006-2007 (Laurens, Minerva), 2009-2010 (New Orleans), and 2012-2013 (Sydney) [65]. This pattern of emergent strains causing large-scale epidemics indicates that Norovirus is currently

undergoing “epochal” evolution, wherein periods of relative stasis are punctuated by stepwise emergence of phenotypically distinct viral variants, a phenomenon first associated with Influenza A virus [65, 66]. The driving forces behind epochal evolution are an increase in viral fitness coupled with selective immune pressure in human hosts. Patients who are chronically infected with human Norovirus act as a reservoir for the pathogen, as they continually shed virus and exert selective immune pressure on the virus, which may mutate substantially over time to evade the immune response [67]. In a study by Nilsson et al., a patient with chronic diarrhea was found to be infected with GII.3 HuNoV, and this virus accumulated 32 amino acid changes over the course of a year [67]. The majority of these mutations arose within the P2 hypervariable domain of the VP1 capsid protein, the primary external domain thought to play a role in HBGA binding and species specificity [67]. The P2 domain of GII.4 Norovirus permits a wider binding to HBGA compared to other genogroups, which in turn increases host specificity for the virus to the point that GII.4 HuNoV can infect all secretors of ABO blood groups [68]. GII.4 HuNoV also has a higher polymerase mutation rate, permitting more rapid evolution than other genogroups [69]. This increased mutation rate coupled with wider host specificity may be the reason for the success of GII.4 as the predominant genotype for HuNoV, responsible for 70-80% of worldwide outbreaks [70]. Donaldson et al. hypothesized that Norovirus capsid evolution is simultaneously driven by evasion of herd immunity and retention of ability to bind HBGA, while Shanker et al. detected no alterations in HuNoV HBGA interactions when 2 residues of the P2 loop were altered in a 2004 Grimsby variant [71]. Lindesmith et al. demonstrated that the primary cause of the 2009 outbreak, GII.4 New Orleans HuNoV, likely arose from the prior outbreak’s cause, GII.4 Grimsby strain, through blockade epitope evolution in an attempt to evade herd-wide immunity among hosts [72].

Disease

Human Norovirus infection typically causes acute gastroenteritis, of which the primary symptoms are nausea, stomach pain, watery diarrhea, and “forceful” vomiting [73]. Other common symptoms include low-grade fever, malaise, headaches, weakness, and loss of taste [73]. Less common symptoms include benign infantile seizures, encephalopathy, and disseminated intravascular coagulation [74]. Severe complications arising from Norovirus infection may include necrotizing enterocolitis of the intestines in premature infants, post-infectious irritable bowel syndrome, and bloody diarrhea in patients with inflammatory bowel disease [75-77].

Onset of symptoms typically occurs within the first 12-24 hours following infection [73]. In healthy adults, the virus is eliminated after only 1-2 days, but symptoms like diarrhea and vomiting may persist for another 1-2 days [73]. In young children and the elderly, disease course may be prolonged, with infections lasting as long as 6 weeks. These groups, as well as the immunosuppressed, are at higher risk of developing complications following Norovirus infection, including dehydration and in the most extreme cases death [78]. In the case of immunosuppressed individuals and transplant patients, Norovirus may not be limited to an acute phase, and may persist as a chronic infection lasting years in some cases [79]. Norovirus was the most common pathogen detected in fecal isolates taken from hospitalized children with primary

immunodeficiencies, with persistent virus shedding in the feces for a median of 9.5 months [79]. In transplant patients, immunosuppression may lead to chronic infection with Norovirus acquired in the hospital setting; up to 20% of allogeneic hematopoetic stem cell transplant recipients developed chronic Norovirus infection in the year following transplant [80]. Nine recipients of kidney transplants were also found to harbor GII.4, GII.7, or GII.17 HuNoV, both symptomatically and asymptomatically, for many years following transplant, which gave the virus time to accumulate up to 25 amino acid variations [81]. This reservoir for virus in the immunosuppressed may facilitate epidemic spread of new HuNoV strains as novel variants arise in chronically infected individuals.

The precise mechanisms by which Norovirus induces vomiting and diarrhea are not well understood. Meeroff et al. identified abnormal gastric function in 1980, featuring delayed gastric emptying presumably due to abnormal gastric motor function, which may contribute to vomiting [82]. Norovirus does not induce diarrhea via widespread damage to the intestinal epithelium, which remains intact throughout the course of infection [83]. Minor histopathological changes during infection were noted by Dolin et al. in 1975, who described a shortening and blunting of the microvilli [83-85]. Intraepithelial cytotoxic T cells were increased in one cohort, but Norovirus generally induces only modest intestinal inflammation [86]. Norovirus does seem to interfere with the proper absorption of various nutrients, inducing malabsoprtion of D-xylose, fat, and lactose as a result of shortened microvilli and decreased brush border enzyme activity [83]. Diarrhea induced by Norovirus does not appear to be a product of intestinal epithelial damage, but may be the result of altered secretory or absorptive processes [87].

Norovirus was once thought to infect enterocytes of the small intestine, though direct experimental evidence to support this claim is lacking. The precise cellular target of Norovirus remains unclear, as electron microscopy of intestinal biopsies in infected volunteers has not revealed virus particles in or on intestinal enterocytes [83, 88]. By comparison, virus antigen was detected in lamina propria cells in biopsies of infected volunteers [89, 90]. In animal models of human Norovirus, including gnotobiotic pigs and calves infected with HuNoV, viral antigen may be detected within enterocytes, suggesting that enterocyte infection in immunocompetent humans is largely controlled through the host immune response [91, 92]. This control of Norovirus may be interferon dependent, as Mumphrey et al. demonstrated that STAT1-dependent interferon responses eliminate clinical disease following MNV-1 infection in mice [93].

Human infection studies have detected viral antigen in the lamina propria of the intestine despite the fact that the epithelial lining of the intestine remains intact; viral antigen in this tissue suggests that Norovirus bypasses the intestinal epithelium via an undiscovered mechanism to infect immune cells [89, 90]. Lamina propria cells and Brunner’s glands, extracted from human intestinal tissue sections, bind viral antigen when incubated with inactivated whole virus [90]. Neither dendritic cells nor macrophages of the lamina propria have been shown to be sufficient to support viral replication *in vitro*. Norovirus may replicate in B cells when infection occurs in the presence of fecal filtrate containing the enteric bacterium *Enterobacter cloacae* [48].

These bacteria express human histo-blood group antigens (HBGAs), a cellular target for viral attachment and entry, and may play a role in both circumvention of the intestinal epithelial barrier and entry into B cells [48].

Host Immune Response

Immunity to human Norovirus is transient and incomplete [73]. In the short term, such as during a single winter outbreak, protective antibodies may provide some resistance to the virus, and repeated exposure to the virus may lengthen the protective duration of these antibodies [94]. In a human challenge model featuring Norwalk Virus, immune protection lasted an average of 6 months following a single exposure [94, 95]. Thorough analysis of immunity to HuNoV is confounded by widespread pre-existing immunity within the population to this ubiquitous virus [2]. In a study by Malm et al., serum from 43 children diagnosed with Norovirus-induced acute gastroenteritis was tested for the presence of pre-existing HuNoV antibodies [96]. Children infected with GII.4 Norovirus exhibited lower levels of antibodies against two GII.4 variants (1999 and 2010) than children infected with other genotypes, offering evidence that serum IgG to GII.4 may offer protection against infection in a genogroup-and strain-specific manner [96]. Following acute illness, all patients seroconverted to the outbreak strain, although seroconversion to other strains was observed at lower frequency [96].

Transmission

Norovirus is transmitted at high efficiency through the fecal-oral route. One common exposure route for the virus is consumption of contaminated food, notably shellfish or fresh produce. Contaminated water, as found in ground wells or unsterilized recreational pools may also harbor the virus. Infectious particles called fomites may be found on shared environmental surfaces, such as toilet handles or elevator buttons; these fomites may be transferred to the mouth and can lead to disease. Finally, virus can be aerosolized by the act of vomiting or via toilet flushes, further spreading infectious fomites to surrounding surfaces [97].

Norovirus is infectious at extremely low doses, with a reported ID_{50} of 18 virions in a human challenge study published by Teunis et al. in 2008 [98]. In this study, the authors diluted 8fIIa Norovirus, the primary inoculum used in the 1971 human challenge experiments by Dolin et al., and 8fIIb, virus derived from the stool of a volunteer challenged with 8fIIa [3, 98]. Virus was quantified by RT-PCR amplification of viral genome, yielding virus concentration measured in genome copies per microliter RNA standard [98]. This quantification method was employed as the 8fIIa virus formed aggregates in the decades of storage since the original study, rendering dilution or sonication ineffective for virus dispersion [98]. Utilizing predictive mathematical extrapolation based on a single hit model for Norovirus infection, Teunis et al. derived a calculated ID_{50} of 1,015 genome copies approximately equivalent to 2.6 aggregated particles [98]. The same method was employed in the dispersed virus to yield a predicted ID_{50} of 18 individual virus particles [98]. Further extrapolation by the authors using this model suggested that even a single virus particle may be sufficient to cause disease in a susceptible individual [98]. Finally, this estimate of Norovirus infectivity

reveals that a majority of Norovirus particles are infectious to susceptible humans, and defective virus is present only as a minor fraction of total virus [98].

A later study by Atmar et al. measured the infectivity of Norovirus and reached a separate conclusion for the ID_{50}. In this study, 57 adult volunteers were recruited and 21 persons were experimentally infected with Norwalk Virus derived from the filtered feces of volunteers previously infected with Norwalk Virus [99, 100]. The study determined the ID_{50} following dilution infections at a value of 1320 genome equivalents in patients with type A or type O blood, higher than the previous estimate and more in line with infectious estimates for other RNA viruses [100]. A rebuttal by Moe et al., however, determined that statistical confidence intervals could not distinguish a difference between the two estimates, and that the true infectious dose of unaggregated virus was not statistically different between these two reports [101].

The extremely low infectious dose of Norovirus facilitates a high attack rate, or mean number of cases following an index infection. Harris et al. reported in 2010 that outbreaks in ships experienced the highest attack rates when compared to other settings, with a median of 237 infected individuals following an index case [102]. Harris et al. also identify nursing homes and hospitals as environments with high median attack rates, 50 and 44 respectively [102]. The attack rate percentage, or fraction of people presumably exposed to the virus who later become infected, was 47.6% across all settings in this study [102]. While staff and crew members were infected at a lower frequency in this study when compared to patients and passengers (34.4%), the implementation of infection control measures did not improve the attack rate percent statistic [102]. Outbreaks where infection control measures were not used featured a 36.1% attack rate (32.4% for staff/crew) [102].

Determining the index case of Norovirus infection, as well as the causative strain and route of subsequent contamination, is difficult because of the widespread concurrent circulation of multiple Norovirus strains during an outbreak. Reservoirs of Norovirus in communities may introduce alternate strains during an outbreak [103, 104]. Exposure to a Norovirus strain associated with severe symptoms increases the likelihood of spread of other Norovirus strains through fomite contamination via vomiting or diarrhea [105]. Additionally, the time to onset of symptoms may vary among patients, rendering identification of an index individual difficult. Finally, even asymptomatic individuals may spread the virus through cross contamination of food or water, as seen in many cases involving food preparation workers on cruise ships or in healthcare settings [105]. In these scenarios, a single individual contaminates food for many individuals, furthering spread at an incredible rate in the enclosed spaces [105].

The most common route for spread of human Norovirus during outbreaks in healthcare settings is direct person-to-person contact with the genogroup II genotype 4 (GII.4) virus [105]. Friesema et al. hypothesized in 2009 that the predominance of GII.4 infections is due to higher attack rates and more symptomatic disease (and thus more fomite contamination) associated with this particular genotype [106]. Additionally, individuals in a healthcare setting are more likely to have pre-existing conditions

rendering them more susceptible to virus infection or less able to clear the virus effectively [105, 107]. In a report by Simon et al. in 2006, an outbreak in a pediatric oncology unit was documented and traced to an index patient [107]. Severe complications arose in three secondary patients, including an 8-month old patient with acute lymphoblastic leukemia who developed bloody stool, a 17-month old boy with Langerhans cell histiocytosis who developed protracted diarrhea, and a 19-year old man with metastatic desmoblastic rhabdomyosarcoma who developed colonic perforation as a result of Norovirus infection [107]. In the case of the 17-month old, shed virus was detected up to 140 days following the infection, suggesting that incomplete clearance of the virus permitted this immunosuppressed individual to serve as a long-term reservoir for the virus [107].

Outbreaks resulting from person-to-person spread are most easily traced to index cases in small, enclosed areas found in airplanes or cruise ships. In 2008, Holmes and Simmons reported that an incident of vomiting during a trans-Pacific flight resulted in acute gastroenteritis in 41 (33.6%) passengers within two seating zones of the index infection [108]. These individuals had no contact with food or water, though some cross-contamination from surfaces in the toilet on board may have aided spread of the virus via fomites [108]. In another report by Kirking et al. in 2010, a flight from Boston to Los Angeles was diverted due to rapid Norovirus outbreak among members of a tour group [109]. Passengers on the flight who were not part of the tour group but sat adjacent to tourists were at significantly greater risk of developing Norovirus infection (7.5 adjusted relative risk) than those who sat further from the index cases [109].

Individuals who prepare food are at particular risk for spreading the virus to a larger group during an outbreak in settings where multiple at-risk individuals are eating collectively prepared food, such as on board cruise ships or in hospitals and restaurants [105]. Sala et al. reported in 2005 on an outbreak caused by food prepared by a symptomatic cook working in a hospital cafeteria [110]. This outbreak, which spread to at least 18 individuals, began when the cook was infected with GI.3 Desert Shield Norovirus after eating at a local seaside restaurant [110]. Two days later, despite developing symptoms including diarrhea and vomiting, this cook prepared food by hand, including sandwiches and salads, which were later identified as the two most commonly consumed items by those who fell ill [110]. Perhaps more alarming are the cases in which infected food handlers remain asymptomatic yet spread the disease to others. In a report by Zomer et al. in 2010, an outbreak involving over 400 office workers in Sweden was caused when an asymptomatic food handler prepared tomatoes for salads and hamburgers [111]. This individual later developed symptoms of Norovirus infection including vomiting, but the previously prepared tomatoes were nevertheless served to the group, resulting in the outbreak [111]. The causative agent in this case was determined to be GI.3 Desert Shield Norovirus and was detected by RT-PCR in the stool of both the index case and secondary cases [111]. In another study by Godoy et al. in 2005, an outbreak of Norovirus was detected in 59 students and teachers staying at a hotel in Spain [112]. In this outbreak, the index case was not identified, though the relative risk for acquiring symptoms was increased following consumption of

sandwiches prepared by two food handlers [112]. Neither of these individuals presented clinical symptoms, highlighting the risk of Norovirus infection despite an apparent lack of a symptomatic index case [112].

Norovirus may be spread indirectly, without a human intermediary, through the consumption of contaminated water or food. Gallay et al. published in 2006 a report detailing an outbreak in France in August 2000 that affected at least 202 residents [113]. During the outbreak in this town, drinking tap water was associated with a three-fold increase risk for illness, and risk directly correlated with amount of water consumed [113]. Subsequent environmental investigation concluded that a groundwater source for the community had become contaminated, and efforts to chlorinate and thus purify the water had failed [113]. The outbreak subsided within a week after the implementation of corrected water control measures [113]. In a report by Podewils et al., an outbreak in Vermont in 2004 was traced to contamination of a swimming pool, resulting in 53 individuals developing diarrhea or vomiting within 72 hours of visiting the pool [114]. In this outbreak, insufficient chlorination and failure to maintain the pool sanitation equipment both contributed to the outbreak [114].

Shellfish, as filter feeders in the ecosystem, are at particular risk of exposure to contaminated fecal samples, a fact that renders them excellent vectors for spread of Norovirus. Burkhardt et al. have demonstrated that bivalve mollusks, like oysters, are capable of bioaccumulation of Norovirus, concentrating the virus 99 times compared to surrounding seawater [115]. Multiple accounts in the literature document outbreaks associated with the consumption of raw shellfish. In an outbreak reported by Ng et al. in 2005, 305 cases of gastroenteritis arose out of 1408 persons who had eaten raw half-shell oysters at multiple restaurants and hotels [116]. Examination of 11 samples of 30 oysters by electron microscopy revealed small rounded particles reminiscent of Norovirus in all 11 samples, though only eight of the 11 samples tested positive by RT-PCR [116]. This outbreak outlined a surveillance deficiency for Norovirus, as shellfish imported from overseas are routinely tested for contamination solely by culturing, a technique incapable of detecting Norovirus [116]. The causative agent for shellfish contamination is usually exposure of the shellfish to raw sewage, as identified in a 2008 Australian outbreak by Huppatz et al. [117]. These outbreaks are not limited to a single production or harvest site, as published by David et al. in 2004, who discovered a widespread pattern of shellfish contamination at 14 geographically dispersed harvest sites throughout Canada [118].

Vegetables and fruit that are irrigated with contaminated water serve as another source of infectious virus [119]. A report by Makary et al. in Finland in 2008 connected an outbreak among 10 workplace canteens to a single vegetable processing plant [120]. This plant supplied raw vegetables to each of the 10 affected canteens, and consuming raw vegetables from this plant was significantly associated with illness at an 82% response rate [120]. Subsequent attempts to track the precise crop responsible for the outbreak were unsuccessful [120]. Another report from Finland by Maunula et al. in 2009 was able to isolate a single crop of raspberries used in cake toppings or chilled cheese curd snacks. These raspberries, which had been frozen for international

shipping, were served without heating and eaten by 30 individuals at a restaurant [121]. One week later, separate raspberries from the original shipment were served to about 90 people at a daycare center [121]. 15 of the 30 patrons of the restaurant developed disease, while 46 patients from the daycare later developed symptoms of Norovirus [121]. The raspberries were tested by RT-PCR and GI.4 Norovirus was identified as the causative agent [121]. Virus was also detected in two fecal samples of infected individuals [121]. A report by Ethelberg et al. identified raw lettuce as another vehicle for Norovirus infection in Denmark in 2010, while reports by Wadl and Gallimore have identified generic salad ingredients as vectors for Norovirus [122-124]. The myriad ways by which this highly contagious virus is transmitted highlight the importance of understanding its basic biology in an attempt to reduce disease transmission.

Decontamination

Norovirus is difficult to inactivate, a factor that permits viral persistence on exposed surfaces and prolongs outbreaks, particularly in enclosed spaces like cruise ships. The virus is presumably not inactivated by freezing, low pH, or alcohol-based disinfectants, based on the physical characteristics of murine Norovirus [125]. MNV and FCV demonstrated resistance to heat killing at temperatures in excess of 60°C, with 30 seconds at 65°C or 11-15 seconds at 72°C required for 1 log reduction in viral titer [126]. MNV is also susceptible to inactivation through exposure to 254nm UV radiation with and without TiO_2, experiencing a 3.6 log reduction following exposure to 25 mJ/cm^2 [127]. MNV and HuNoV VLP are resistant to inactivation via gamma irradiation. The FDA has approved irradiation doses of 4.0kGy to control food-borne pathogens in produce, but MNV-1 only experienced a 1.7-2.4 log virus reduction when exposed to 5.6kGy gamma irradiation [128]. HuNoV may be removed from water using a coagulation-rapid sand filtration process, which demonstrated a 3 log reduction in recombinant HuNoV VLPs at a dose of 40 μM pH6.8 polyaluminum chloride and pH 5.8 ferric chloride [129]. High pressure processing (HPP) has been experimentally employed to inactivate the virus in and on shellfish as well as fresh produce, and a 5 log reduction in MNV-1 resulted following pressurization at 400 MPa for 2 minutes at 4°C [130]. HPP does have an effect on the texture and taste of the treated food items, which hinders its widespread use in the fresh food industry, but offers a method of Norovirus inactivation for processed or frozen food [130]. Contrasting reports exist on the ability of alcohol-based cleaning products to reduce Norovirus infectivity; Park et al. published in 2010 that ≥70% ethanol and isopropanol reduced MNV infectivity by 2.6 logs, while Liu et al. published in 2015 that ethanol based disinfectants were mildly effective at inactivating Norwalk Virus (0.81 +/-.57 log reduction) but had virtually no effect on GII.4 Norovirus (0.14 +/- .13) [131, 132]. Liu et al. further demonstrated that among 12 common cleaning products, bleach exhibited the best ability to inactivate both NV and GII.4 HuNoV, with a 4.84+/-.03 and 3.74+/-.05 log reduction respectively [132]. Hypochlorous solution in a weak acid reduced MNV-1 titer measured by plaque assay, but failed to eliminate infectious virus in the feces of mice that drank the disinfectant [133]. Hydrogen peroxide vapor treatment of multiple surfaces was effective in reducing FCV titer by 4 logs within 20 minutes, which may promote its use in sterilization of surfaces in healthcare settings [134]. MNV is inactivated through exposure to 1mg/liter ozone for 2 minutes, though RT-PCR analysis does not always align with reduced viral

titer as measured by plaque assay [135]. Both peracetic acid and glutaraldehyde reduced MNV-1 titer by at least 4 logs within 5 minutes [136]. Quaternary ammonium compounds are also efficient at reducing viral titer of FCV by 6.4-6.6 logs after 10 minutes of contact [137]. Liquid soap is relatively ineffective, as washing hands with antibacterial soap reduced virus genomic copies by only 0.6-1.2 log, compared to 0.58-1.58 log through water rinse alone [138].

Host Specificity

Human Norovirus binds to the polymorphic histo-blood group antigens (HBGAs) during infection. HBGAs are a collection of uncharged sugar residues containing structurally related saccharide moieties, ABO antigens, and Lewis antigens, most commonly associated with the ABO antigens that determine an individual's blood type [48]. A large number of alternate antigens are derived from the precursor molecules to the O antigen, namely Galβ1-3GlcNAcβ or Galβ1-4GlcNAcβ. These carbohydrate moieties are modified through the addition of a fucose residue to the terminal galactose residue via α1,2 linkage with α1,2 fucosyltransferase FUT1 or FUT2 [139]. FUT2 is of critical importance for Norovirus binding, and Lindesmith et al. have demonstrated that FUT2 deficient individuals, known as secretor negative and accounting for approximately a fifth of the population, are resistant to Norovirus infection [139].

HBGAs are expressed on the surfaces of epithelial cells, are secreted extracellularly in saliva, and are secreted by certain enteric bacteria to form a "highly hydrated biofilm matrix," commonly observed in wastewater sludge [140]. In some cases, enteric bacteria may display the human-encoded antigens [48]. Due to the role of the ABO antigens in blood grouping and in Norovirus infection, many hypothesized that certain blood groups might confer resistance to HuNoV [141]. In a report by Hennessy et al. in 2003, the B type blood antigen was hypothesized to confer resistance to human Norwalk-like virus infection, though the analysis of a cohort in a British military field hospital in Bagram, Afghanistan did not have sufficient numbers to fully power a statistically significant difference [141]. In this case, a blood type of O was associated with an odds ratio of 1.41 (0.71-2.79 95% CI), type A was associated with 1.10 OR (0.40-3.01), and type B with an OR of 0.15 (0.00-1.27) [141]. Finally, individual Norovirus molecules may associate with varying HBGAs during passage through the host [71]. Shanker et al. constructed a predictive model suggesting that a single Norovirus particle may bind to salivary HBGAs, become ingested, and then bind separate HBGAs located on the intestinal epithelium to commence productive infection [71].

Diagnosis

Norovirus is an exceedingly common virus, affecting around 267 million individuals each year and leading to more than 200,000 deaths worldwide annually [11]. Death from Norovirus is uncommon in developed countries and healthy individuals; the most common victims to succumb include the young, the elderly, or the immunocompromised [11]. In the US, Norovirus leads to between 19 and 21 million infections per year with 1.7-1.9 million outpatient visits and 400,000 emergency department visits, resulting in between 56,000 and 71,000 hospitalizations and between

570 and 800 deaths [11]. The estimated lifetime risk of death is therefore low, 1:5000 to 1:7000, but the risk of contracting Norovirus is high, with a predicted 1:0.2 lifetime risk corresponding to an average of five infections per lifetime [11].

Diagnosis of Norovirus is reliant on RT-PCR amplification of viral genetic material, as no *in vitro* culture system exists for the virus. Jiang et al. were the first to describe RT-PCR amplification of Norovirus genetic material from the stool of patients suffering from acute nonbacterial gastroenteritis [8]. Modifications of this initial protocol serve as the basis for most modern surveillance and diagnostic efforts focused on Norovirus.

Surveillance

Despite Norovirus's status as a common cause of human disease, less focus has been applied to detection of the virus when compared to enteric bacteria and other causes of gastroenteritis. The lack of a tractable culture system for Norovirus has long hindered the detection of this pathogen, and the application of RT-PCR to detect the virus has only existed for the last decade of the 42 years since the virus's discovery [8]. Prior to the adaptation of RT-PCR to Norovirus, electron microscopy was utilized to observe the small rounded particles associated with nonbacterial gastroenteritis [2]. With the addition of RT-PCR to the repertoire, most outbreaks of acute gastroenteritis are now screened for the presence of Norovirus genetic material.

Rapid detection of Norovirus outbreaks permits the implementation of control measures that may halt the spread of the virus. To that end, in 2009 the Centers for Disease Control and Prevention (CDC) launched the National Outbreak Reporting System, or NORS, to collect information on enteric diseases including Norovirus [10]. This system is a voluntary participation system, with local public health agencies reporting outbreaks over the Internet. Another detection program is the CaliciNet, also launched in 2009. This program seeks to compare strains of current outbreaks with archived genetic sequences to monitor presently circulating virus and rapidly detect newly emerging strains. Finally, the CDC operates the Norovirus Sentinel Testing and Tracking network, or NoroSTAT, which began in 2012. This program is a network of state health departments working in conjunction with the CDC to establish standard operating procedures following Norovirus outbreaks.

European countries have similar programs in place to combat the spread of Norovirus. The European Centre for Disease Prevention and Control works with the journal Eurosurveillance to document the spread of Norovirus during European outbreaks. This journal provides rapid in-depth reports on outbreaks that occur, facilitating the rapid responses necessary to withdraw contaminated food from the market following identification of Norovirus. The Foodborne Viruses in Europe (FBVE) network is a joint database whose function is to aggregate and share epidemiological and virological outbreak reporting [70]. In the Netherlands, Noronet is an extension of the FBVE network, a collection of virologists and epidemiologists founded in 1999 that seeks to share and maintain information regarding prevailing Norovirus outbreaks.

Treatment

Treatment for infected individuals is limited to palliative care and rehydration to combat fluid loss from diarrhea [11]. There is currently no known cure for Norovirus, other than letting the virus run its course [11]. No specific antivirals are prescribed to combat Norovirus, as the infection is typically acute and self-limiting in nature [11].

Efforts in the public health sector are primarily focused on combating Norovirus through the prevention of spread [11]. The suggested guidelines for stopping the spread of Norovirus call for frequent hand washing, thorough rinsing of fruits and vegetables with fresh water, cooking shellfish thoroughly, cleaning surfaces and washing laundry with chlorine-based disinfectants, and avoiding preparing food if symptomatic or currently infected [11].

Vaccine Prospects

There is currently no licensed vaccine for Norovirus, despite substantial economic incentive. Bartsch et al. predicted that a vaccine with 50% efficacy rate that induces only 12 months' immunity, rather modest endpoints for a vaccine, could prevent between 1 and 2.2 million HuNoV infections annually in the US and aid in the recovery of the $2.1 billion lost as a result of decreased productivity following infection [142]. Because of the difficulty of culturing Norovirus *in vitro* and a lack of suitable small animal models, vaccine development for Norovirus has focused on particle vaccines rather than live-attenuated virus. The most common approach for vaccine development is the generation of virus-like particles (VLPs). These particles consist of the major capsid protein VP1 assembled into the virion shell, but lack a functional genome, rendering them non-infectious [143].

In a study by Hale et al. in 1999, viral genetic material was purified from stool samples of a patient infected with Grimsby GII.4 Norovirus, the predominant strain in the United Kingdom during the winter of 1995-1996 [143]. The RNA was converted to cDNA through reverse transcription and the resultant cDNA was utilized to determine the sequence for the major capsid protein VP1 via nested PCR amplification [143]. The determined 1.6kb VP1 sequence was cloned into a recombinant "bacmid" vector featuring a polyhedron promoter using a baculovirus shuttle vector with a helper plasmid in *E. coli* [143]. This construct was then transfected into *Spodoptera frugiperda 9* (Sf9) cells, a cell line derived from the ovaries of a Fall Armyworm [143]. VLPs were isolated from the transfected cells via ultracentrifugation and sucrose gradient purification [143]. This system serves as the basis for the majority of VLP recovery techniques in the field to date.

El-Kamary et al. performed a phase I clinical trial to evaluate the safety of GI.1 VLPs prepared using this baculovirus system. The results, published in 2010, indicated that the VLPs are safe for human intranasal administration [144]. In this study, VLPs were adjuvanted with four components: monophosphoryl lipid A, TLR-4 agonist derived from the LPS of detoxified *Salmonella Minnesota* bacteria, chitosan derived from shrimp shells, a mucoadhesive designed to prolong antigen adherance in the nose, and the bulking agents sucrose and mannitol excipients, which serve to preserve VLP structure

during lyophilization [144]. Two doses of this dry powder, separated by 21 days, were administered instranasally into each nostril of twenty-eight randomized 18-49 year old volunteers in a dose-response experiment [144]. A follow-up study in the same paper followed 61 adults given an even higher intranasal dose of 100μg again in duplicate and separated by 21 days, and immunogenicity, symptoms, and adverse effects were measured and compared to placebo treatment [144]. At the highest treatment dose, 63.2% of subjects experienced a greater than four-fold rise in geometric mean titer of total antibody to GI.1 Norovirus compared to 9.1% in the placebo, indicating sero-response [144]. Furthermore, the ability of Norovirus-specific antibody producing cells to home to the intestine was measured by staining PMBCs from 5 subjects and sorting these cells into subsets based on mucosal homing markers [144]. The majority of IgA secreting cells, which are presumably protective against Norovirus, were positive for the gut-homing molecule $\alpha4\beta7$ integrin, indicating a preference for intestinal localization [144]. Adverse effects of the vaccine were primarily localized in the nose, including nasal stuffiness, discharge, itching, and sneezing, with a few reports of bloody mucus [144]. These symptoms were also seen in the adjuvant alone group, but were not as frequent in the placebo treatment [144].

A more recent phase 1 clinical trial conducted by the Takeda Corporation (previously Ligocyte) demonstrated safety of a bivalent Norovirus VLP vaccine candidate [42]. In this study by Treanor et al. in 2014, 48 adults between the ages of 18 and 49 were injected with two doses of up to 150μg GI.1 VLP and a consensus GII.4 VLP adjuvanted with monophosphoryl lipid A and alum or placebo 28 days apart [42]. This dose escalation study was followed in the same publication by injection of 54 subjects in different age groups at the 50μg dose [42]. The vaccine candidate induced no illness or fever, and there were only mild reported adverse events, mainly pain associated with the intramuscular injection or mild headache [42]. Furthermore, vaccinated individuals mounted significant immune responses to the GI.1 VLPs at all doses in excess of 5μg compared to the placebo [42]. Responses to the GII.4 consensus VLPs were variable, with only 56% of subjects responding at the lower doses, increasing to 75-88% responding at the higher doses [42]. In both cases, the secondary immunization did not elicit a stronger response as measured by geometric mean titer of total immunoglobulin to Norovirus GI.1 and GII.4 [42]. These responses were detected in wild-type individuals as well as those lacking a functional FUT2 gene, or secretor negative individuals, who are generally considered resistant to infection by Norovirus [42]. Furthermore, immunity as measured by geometric mean antibody titer appeared to be fairly transient, as titers significantly declined in the 393 days following immunization [42].

A subsequent randomized, double blind challenge study with this VLP candidate vaccine failed to meet a pre-defined primary experimental endpoint [145]. FUT2 competent (and thus Norovirus-susceptible) volunteers were vaccinated with two injections of 50μg GI.1 and GII.4 VLPs derived from a baculovirus expression system and adjuvanted with monophosphoryl lipid A and alum 28 days apart [145]. 109 subjects were then admitted to an inpatient challenge facility and dosed with $4.4x10^3$ RT-PCR units of a Norovirus strain derived from a 2003 clinical sample from the GII.4

Farmington Hill outbreak [145]. Challenge occurred between 42 and 196 days post-infection [145]. All volunteers mounted a serum response to GI Norovirus after a single dose of the vaccine, while only 83.7% mounted a serum response to GII Norovirus after a single dose, and 89.8% after a second dose [145]. Unfortunately, the vaccine did not significantly reduce the incidence of illness, with 13 of 50 vaccinees and 16 of 48 placebo recipients developing illness following challenge [145]. While incidence was unaffected, severity of symptoms appeared to follow a decreasing trend following vaccination. Analysis of the total incidence of vomiting or diarrhea of mild or greater severity indicated a significant reduction in vaccinees compared to placebo recipients [145]. This mild effect, coupled with the transient nature of immunity to Norovirus elicited by the vaccine, shows that the field has much farther to go before a reliable vaccine against Norovirus is available.

Culture Systems

Until very recently, there has not been a tractable model for culturing human Noroviruses in any known cell type or line. One attempted approach for culturing the virus involved a 3D intestinal cell culture system. In this system, Int-407, a HeLa contaminated intestinal epithelium cell line derived from the jejunum and ileum of a 2-month-old Caucasian embryo, or Caco-2 cells, a colonic epithelial cell line derived from a 72-year old Caucasian male, were grown for 4 weeks while rotating in a “bioreactor” meant to simulate conditions found within the human gut. Once differentiated, cells were transferred to tissue culture plates and infected with fecal filtrates lacking any bacteria but containing a number of genotypes of human Norovirus. Despite successful differentiation of the gut cells, no significant replication of human Norovirus RNA was detected in any genotype of virus or in any cell line [146].

Jones and colleagues were the first to describe a cell culture model featuring RNA replication *in vitro* in November of 2014 [48]. This major breakthrough demonstrated infectability of a Burkitt’s lymphoma cell line with human Norovirus in the presence of the enteric bacteria *E. cloacae* [48]. In this report, the researchers first determined if the surrogate MNV-1 could infect B cells of mice. To that end, M12 and WEHI-231 cells, both murine B cell lymphoma cell lines, were infected with either MNV-1, which establishes an acute infection similar to Norovirus, or MNV-3, which establishes a persistent, attenuated infection. In both cases, MNV replicated efficiently in the B cell lines with viral titer peaking at 2-3 days post infection [48]. The B cells died as a result of infection, but the major capsid protein VP1 was observed in cell lysate, indicating that viral protein synthesis was occurring [48]. Jones et al. expanded this observation to observe the infectivity of a human B cell line by human Norovirus. GII.4 Sydney Norovirus, the current prevailing strain, was inoculated onto BJAB cells either directly or following filtration through a 0.2μm filter [48]. In the unfiltered inoculum, the initial dose of 10^6 genomes/well increased 25-fold after 5 days of culture [48]. This genome replication was significantly greater than filtered virus, which only saw a modest half-log increase of viral genetic material [48]. This increase was ablated following UV-inactivation of the virus, and HuNoV protein expression was detectable from 3-5 days post-infection in the unfiltered inoculum [48]. Jones et al. isolated the filtered element responsible for increasing infectivity of the HuNoV inoculum and identified the enteric

bacteria *E. cloacae*, which enhanced Norovirus infectivity with affinity equal to the synthetic H-type histo-blood group antigen, as well as the positive control of unfiltered stool [48]. *E. cloacae* itself expresses the human histo-blood group antigens which act as adsorbents for human Norovirus [147]. The virus binds to extracellular polymeric substances on the surface of the bacteria, in areas of concentrated HBGA [147].

Animal Models

Animal models for human Norovirus are hindered by the virus's extreme species specificity. Noroviruses bind the human histo-blood group antigens, which renders them primarily infectious to humans. As most other species have dissimilar HBGAs, Norovirus is less able to infect animals when used to model the human disease.

The most tractable small animal model to-date for human Norovirus involves humanized mice as described by Taube et al. in 2013 [148]. In this report, the authors reconstituted the immune system of BALB/c mice deficient for the recombination activating genes RAG1 and RAG2 as well as the common gamma chain (γC) using CD34+ hematopoietic human stem cells. After six months, these humanized mice were then infected with either GII or GI and GII Norovirus simultaneously via intraperitoneal injection of 0.2 mL sterile-filtered stool suspension as well as orally with 0.05 mL clarified, unfiltered human stool suspension. Both humanized and RAG/γC deficient mice were susceptible to subclinical infection of HuNoV as measured by increases in genomic RNA compared to input as well as expression of viral capsid protein in infected cells [148]. Virus genome was detected in the stomach, jejunum/duodenum, proximal and distal ileums, cecum, colon, mesenteric lymph nodes, liver, kidney, heart, lung, and bone marrow at 24 hours post-infection (hpi) [148]. By 72 hpi, only GII virus was detectable in the humanized mice in the jejunum/duodenum, proximal ileum, and cecum [148]. Between two and six $\log_{10}$ virus was detectable in all conditions within 24 hours post-infection, with most virus cleared by 72 hours post-infection [148]. One mouse with high titer developed watery diarrhea [148]. There was no statistical difference between the immune deficient mice and the humanized mice, suggesting that possessing human immune cells is not a prerequisite to Norovirus infection [148]. Among the humanized mice infected with a GI and GII mix, no GI virus was detected in any tissues or feces [148]. Humanized mice were also infected purely via the intraperitoneal route; this route gave similar infectivity to the IP/oral challenge for the GII strain [148]. The GII virus did not undergo mouse adaptation as measured by 454 sequencing, with only 2 silent mutations detected [148]. Using antibodies to nonstructural proteins as well as the major capsid protein VP1, histopathological analysis of the tissues of infected mice indicated that the virus infects macrophage-like cells in the small intestine, spleen, and liver [148]. All of these data suggest that viral protein is being produced in this mouse model, which may permit study of the virus life cycle. The pathology of the disease in mice is different from humans, however, and conclusions from this model regarding the progression of disease should be drawn with caution.

A study by Cheetham et al. in 2006 evaluated gnotobiotic pigs as a suitable animal model for human Norovirus [91]. 65 germ-free or gnotobiotic pigs were inoculated with serial passages of a fecal filtrate taken from a child patient with diarrhea

[91]. This inoculum contained 5.4 x 10^6 genomic equivalents per mL of GII.4 HS66 human Norovirus as measured by RT-PCR [91]. 37 pigs received intra-oral inoculation of 1:10 diluted passage 0 filtrate, while 18 pigs received intestinal contents of the P0 inoculated pigs (P1), and 10 pigs received intestinal contents of the P1 inoculated pigs (P2) [91]. Titer of virus genome equivalents decreased after each passage through the pigs, with the initial input titer of 5.4 x 10^5 decreasing to 1 x 10^2 in P1 and 0.8 x 10^1 by P2 [91]. 48 of the 65 P0 pigs developed mild diarrhea compared to 0 pigs in the mock group[91], while 29 of the 65 P0 pigs shed virus in the feces as detected by RT-PCR [91]. HuNoV capsid proteins were detected in the small intestinal tissues by immunoflourescent microscopy, but the decreasing genomic titer suggests that the virus is failing to replicate in this animal model, which limits its use in tracking the virus life cycle.

Animal models in chimpanzees and rhesus monkeys have also been attempted with limited success, but these models are restricted by ethical considerations and decreased funding to chimpanzee research [149]. In 2002, Subekti et al. published a report detailing infection of newborn pigtailed macaques with a Norwalk-like virus Toronto virus P2-A [91]. Monkeys were infected via nasogastric tube and developed symptoms characteristic of Norovirus infection, including diarrhea, dehydration, and vomiting [91]. Further, viral RNA was detected following RT-PCR analysis of RNA extracted from stool samples in all infected monkeys [91]. In a 2005 report, oral inoculation of Norwalk Virus in common marmosets and cotton top tamarins but not cynomolgus macaques resulted in low levels of viral replication as measured RT-PCR performed on fecal isolates [150]. Total amount of virus detected in feces, which peaked at a maximum of $10^{4.4}$ PCR-detectable units (pdu)/g feces, did not exceed input titer [150]. None of the primate species developed diarrhea, lost weight, or had changed behavior (including food intake) following infection [150]. Rhesus macaques, as demonstrated in the previous report, shed virus from 1-2 days post inoculation, with one animal shedding up to 19 days post-inoculation, suggesting that rhesus macaques may provide a limited albeit expensive model system [150].

Surrogate Virus Models

In the absence of a tractable small animal model for the study of human Norovirus, researchers have relied on surrogate viruses similar to human Norovirus. These caliciviruses presumably share similar biological features with human Norovirus and have animal hosts that permit ethical study of the virus life cycle. The oldest and perhaps best studied of these models is Murine Norovirus, or MNV. Karst et al. identified a strain of MNV, MNV-1, in mice deficient for RAG2 and signal transducer and activator of transcription 1 (STAT1) [151]. Homologous sequences to calicivirus genomes were acquired using representational difference analysis, and virus presence was confirmed using electron microscopy [151]. These viruses were demonstrated to be susceptible to interferon signaling in mice deficient for IFN-$\alpha\beta$R and IFNγR, but not adaptive immune responses (RAG$^{-/-}$).[151] In three RAG-deficient mice infected with MNV-1, virus was detected in the lung, liver, spleen, intestine, and blood [151]. Target cells infected with MNV-1 appeared to be primarily innate immune cells, notably macrophages and dendritic cells [151]. In two RAG/γC$^{-/-}$ mice infected via the peroral

route, virus was detected in the brain, while low titers of shed virus were detected in the feces of one mouse infected intranasally and one mouse infected perorally [151]. These viral populations were not necessarily considered physiological due to the global immunosuppression of RAG/γC deficient mice [151]. Substantial tissue pathology was observed following infection in STAT1-deficient mice, though no symptoms of severe diarrhea were reported [151]. As mice lack the ability to vomit, this particular symptom cannot be analyzed using this model.

A conflicting report published by Shortland et al. in 2013 details a MNV-1 variant (dubbed MNV-O7) that is cleared only when STAT1 is deficient and remains persistently infectious in wild-type mice [152]. This virus produces only subclinical infection, perhaps mimicking strains of Norovirus that infect resistant members of the population and thus go undetected [152].

MNV shares features with human Norovirus that increase its use as a model for studying the life cycle, if not the pathogenesis, of the human virus. One of the first discovered features shared between these two viruses is the utilization of subgenomic RNA for the synthesis of viral capsid protein [153]. Subgenomic RNA between MNV and HuNoV share sequence homology at the 5' end, a feature later understood to be important for VPg conjugation [153]. MNV-1 also rearranges intracellular membranes during replication similar to feline calicivirus, a vesivirus and member of the *Caliciviridae* family. In addition to membrane rearrangement, a further characteristic of cells infected with MNV-1 is the arrest of cell cycle in the G0/G1 phase [154]. When MNV-1 was propagated in RAW264.7 cells, cell cyclin levels, notably Cyclin A, were altered compared to mock infection, resulting in a failure to transition to the S phase of replication [154]. Furthermore, when synchronized cells were infected with MNV-1, cells in the G0/G1 phase produced twice as many virions as asynchronous infected controls.[154]

Murine Norovirus 1 utilizes the eukaryotic initiation factor 4E, a limiting factor in cellular translation, to aid in translation of the viral proteins [29, 30]. This hijacking of cellular machinery is due to the actions of the viral protein, genome-linked (VPg), one of the proteins derived from the first open reading frame of MNV-1 [30]. In a report by Chung et al. in 2014, VPg was shown to interact with the eIF4F complex by binding eIF4G, while a follow-up study by Royall et al. in 2015 demonstrated that inhibition of the eIF4E-eIF4G complex using a specific inhibitor reduces MNV-1 replication in RAW264.7 cells [29, 30].

Another model virus used is the Tulane virus, first isolated in 2008 by Farkas et al. from stool samples of juvenile rhesus macaques housed in the Tulane National Primate Research Center [155]. This virus which naturally infects primates bears significant similarities to human Norovirus, and was shown to induce diarrhea, fever, and inflammation of the duodenum in two of three juvenile rhesus macaques following intrastomacheal inoculation [156]. The virus also recognizes histo-blood group antigens in a manner similar to those recognized by human Norovirus [157]. In a study by Zhang et al. in 2015, Tulane Virus was shown to bind to type 3 of the HBGA A antigen as well

as all four of the B antigens tested [157]. Tulane virus does not share all of the properties of human Norovirus, however, as demonstrated by Hirneisen et al. in 2013 [158]. In this report, the authors compared various inactivation treatments on Tulane Virus and MNV-1 to determine which model would better serve as surrogate for human Norovirus [158]. While there was no significant difference between viruses with regard to heat inactivation, extreme pH values and high chlorine concentrations inactivated Tulane Virus more than MNV, suggesting that MNV behaves more similarly to the stable human Norovirus [158].

Reverse Genetics

A robust reverse genetics system for human Norovirus has proven fairly elusive, in part because of the inability to culture any rescued virus. The ability to generate *de novo* virus from cloned cDNA offers a unique approach to studying the virus, and a robust reverse genetics system would greatly aid in improving our understanding of this important pathogen [159]. Initial forays into the reverse genetics of caliciviruses revealed that RNA derived from cDNA clones of feline calicivirus was not infectious in the absence of VPg unless capped with a 5' methyl$_7$G cap [26]. A complete rescue system for FCV was first described in 1996 utilizing transfection of a full-length cDNA genome under control of a T7 promoter to recover infectious virus [160]. A similar system was described in 2005 for porcine enteric calicivirus, though this rescue was dependent on the presence of bile acids [161]. In 2007, a system for the recovery of MNV was described featuring transfection of a consensus sequence of passage 3 MNV-1 CW1 strain genome downstream of a T7 promoter [162]. When T7 polymerase was supplied via co-infection with a T7-encoding vaccinia virus, no virus was recovered, but an alternative source of T7 derived from fowlpox virus proved effective in recovering virus at 5.12 x 10^6 $TCID_{50}$ [162]. Rabbit hemorrhagic disease virus was successfully recovered following transfection of a full-length cDNA plasmid under control of the eukaryotic cytomegalovirus promoter in a VP2 independent manner [163]. The primate calicivirus Tulane virus was successfully recovered following transfection of *in vitro*-transcribed RNA from a full-length genomic cDNA template into permissive LLC-MK2 (rhesus monkey kidney) cells [164]. This RNA was only infectious when capped during the RNA transcription reaction using a methyl$_7$G cap [164]. Methyl$_7$G or VPg 5' capping is not an absolute requirement of caliciviruses, as MNV and FCV may both be recovered from plasmids encoding encephalomyocarditis virus internal ribosomal entry sites (EMCV IRES) [165].

The first reported system for rescuing human Norovirus was published by Asanaka et al. in 2005, wherein cDNAs encoding Norwalk Virus genomic and subgenomic RNA were transfected into mammalian cells, resulting in translation of viral protein and release of virus particles [19]. In this report, the authors assembled DNA constructs featuring the genomic and subgenomic coding sequences of GI.1 Norwalk Virus under control of a T7 promoter sequence. These sequences were followed by a downstream 3' poly-A (26) tract, a hepatitis delta virus ribozyme (HdRz) sequence, and a T7 terminator sequence. This design permits self-cleavage of the RNA downstream of the 3' end of the poly-A tract, leaving RNA corresponding to the natural viral RNA. To rescue virus from these two constructs, the human embryonic kidney cell line HEK293T

cells were infected with a modified vaccinia Ankara strain encoding T7 polymerase (MVA-T7) at a multiplicity of infection of 10 $TCID_{50}$. After incubation for one hour at 37°C, cells were transfected using Lipofectamine 2000. The T7 polymerase supplied by the MVA-T7 then transcribed the viral RNA, which was translated by the HEK293T cell machinery to give rise to viral protein expression, specifically Pro and Pol as measured by radioimmunoprecipitation as well as immunofluorescence [19]. Furthermore, viral capsid protein VP1 was translated from the subgenomic RNA and detected by these same two methods, and this protein was able to polymerize to form capsids detectable by electron microscopy following filtration to remove MVA-T7 and isopycnic CsCl gradient centrifugation [19]. Unfortunately, this viral particle generation occurred at fairly low efficiency, with 12 75cm^2 flasks required for each round of rescue [19]. The rescued virus was not tested for infectivity in humans, and no use of surrogate animal models was reported.

This initial approach was followed by a similar tactic in an attempt to rescue a genogroup II HuNoV, a more relevant disease model. Katayama et al. published in 2006 that T7-driven transcription of RNA from a full-length cDNA clone encoding GII.3 U201 Norovirus, a member of the Mexico cluster of HuNoV, enables virus rescue [166]. This full-length clone was transfected into HEK293T cells infected with Vaccinia virus encoding T7 polymerase and virus protein expression was observed by western blot. When ORF1 was transfected alone, only nonstructural proteins and not VP1 or VP2 were detected in cell lysate, suggesting that the virus life cycle was not running to completion [166]. When the subgenomic sequence was expressed *in trans* in a second plasmid, virus capsid proteins were expressed as observed by western blotting and electron microscopy, though negative staining of the inner portion of the viral particles suggested that these virions comprised only capsid and not other viral products [166].

This model was adapted in 2014 in an attempt to rescue virus from a single transfected plasmid, an approach that did not work in 2006 [167]. In this report, full-length GII.3 U201 HuNoV cDNA was placed under control of an EF-1alpha promoter rather than a T7 promoter, with the goal of permitting rescue in any transfected mammalian cell [167]. The authors noted that previous attempts to use a CMV promoter were unsuccessful [167]. In addition to the basic U201 virus, clones encoding viral variants with exogenous fluorescent reporter genes at different positions in the genome were also assembled to probe the virus life cycle [167]. When transfected into COS7 cells, an African Green monkey fibroblast-like cell line expressing the SV40 T antigen, these clones drove transcription of the viral polyprotein, which was catalytically active and auto-cleaved into the six nonstructural viral proteins as measured by western blotting and immunofluorescent staining [167]. These proteins were observed throughout the cytoplasm of the transfected cells in a diffuse manner [167]. When a point mutation was inserted into the viral protease, expression of the cleaved products NTPase and 3A-like protein was lost [167]. Intact virions were purified using CsCl gradient centrifugation in the supernatant of transfected cells, but these virions were not assayed for infectivity [167]. Progeny virus was shown to contain full-length genomic Norovirus RNA as measured by northern blot [167].

Conclusion

Norovirus is a primary cause of acute viral gastroenteritis worldwide, and leads to a significant healthcare burden in the United States. The term “Norovirus” comprises multiple viruses similar to the prototypical Norwalk Virus, first isolated in 1972 from an outbreak in Norwalk, Ohio. This genus of viruses features small, rounded viruses encoded by a 7.3-7.5 kb nonsegmented single stranded RNA genome with three open reading frames encoding at least eight protein products. Little is known about the virus life cycle, and the functions of at least two of the proteins encoded by the virus have no known sequence or functional homology to any cellular or virus protein. Norovirus is easily transmitted within the human population, particularly in enclosed spaces such as hospitals and cruise ships, and has led to at least six major epidemics in the past twenty years as the virus undergoes epochal evolution to escape herdwide immunity.

Acquired immunity to Norovirus is incomplete and transient, despite nearly ubiquitous exposure to this pathogen, for reasons that are not well understood. Despite the enormous health and economic burdens associated with Norovirus-induced gastroenteritis, our basic understanding of Norovirus biology has lagged behind that of other viruses due to a lack of tractable culture and animal models. There is no licensed vaccine or treatment available for Norovirus despite a recent clinical trial that resulted in modest reduction of major symptoms. A tractable rescue system for human Norovirus offers a valuable tool to study the biology of this virus. The two currently published rescue systems for GI.1 and GII.3 Norovirus are limited in their protein expression and rescue efficiency, and even minor improvements would greatly increase the feasibility of these systems. Adapting the published rescue systems for human Norovirus to the clinically relevant GII.4 strain and increasing the rescue efficiency of the resultant system is of great importance in furthering our understanding of this human pathogen.

Chapter 2
Adapting Published Rescue Systems to GII.4 New Orleans Human Norovirus Using 5' Ribozyme Sequence, Increased Poly-A Tail Length, and Human Codon Optimization

Introduction

To date, no rescue system has been demonstrated for GII.4 human Norovirus (HuNoV). Published methods for the rescue of HuNoV are limited to the GI.1 and GII.3 strains at fairly low efficiency compared to other viruses [19, 166, 167]. These viral genogroups constitute only a minority of Human Norovirus-associated disease; the GII.4 strain has quickly eclipsed other genotypes to become the prevailing strain and is associated with 70-80% of Norovirus infections worldwide [72, 168]. Adapting the published rescue systems to a GII.4 viral variant would offer a novel approach to studying the genetics of the causative agent for acute viral gastroenteritis and would aid in our general understanding of this important human pathogen.

The three published systems for HuNoV rescue feature only modest genomic replication and low protein expression. In the first report on the recovery of GI.1 Norwalk HuNoV, Asanaka et al. required transfection of 12 75cm^2 flasks per round of rescue in order to recover measurable protein [19]. Viral protein detected by immunofluorescence in transfected cells was only observable at low frequency and low intensity, suggesting a paucity of protein translation [19]. RNA packaging in assembled virions was detected, but replication of HuNoV RNA was not determined in this report. Virus assembly and packaging was only detected in those cells transfected with both genomic and subgenomic cDNA but not genomic cDNA alone, indicating that the virus was not transitioning through its life cycle [19]. Furthermore, VP1 and VP2 protein expression were not detected in cells transfected with genomic cDNA alone, despite confirmed expression of nonstructural proteins as well as low transcription of subgenomic RNA from the genomic template [19]. These factors suggest that virus protein expression or function is inefficient in this model, as each component believed to be necessary for viral replication was present in this study yet the viruses failed to transition through the full life cycle [19].

Katayama et al. published a similar approach to the rescue of GII.3 U201 HuNoV wherein protein expression following genomic cDNA transfection was similarly inefficient [166]. In this report, like the 2005 Asanaka paper, RNA of the predicted size was synthesized from both genomic and subgenomic transfected cDNA, yet protein expression was inefficient when genomic cDNA was used as the template [19, 166]. This report featured strong, widespread expression of VP1 when subgenomic RNA was transfected, demonstrating the potential for virus protein expression from a plasmid [166]. Only extremely modest VPg expression was observable near the nucleus of cells transfected with genomic cDNA, and while intensity increased in the 72 hours following transfection, no VP1 or VP2 was ever detected. This failure of VP1 translation again indicated a functional breakdown in the virus life cycle [166].

Due perhaps in part to this low protein expression of HuNoV nonstructural proteins, in 2014 Katayama et al. published a modified approach to rescue GII.3 HuNoV [167]. This system makes use of the eIF1a promoter rather than the original T7 promoter, with the goal of increasing protein expression and permitting the use of other host cells [167]. This publication features the most thorough description of the three published systems due to its analysis of protein expression and function following initial transfection. The authors demonstrate clear expression and cleavage of the nonstructural polyprotein using antibodies to each of the individual constituent proteins in both western blotting and immunofluorescence [167]. Subgenomic RNA was produced by the functional and cleaved RdRP as observed in the 2006 Katayama report [167]. The 2014 paper was the first to demonstrate, however, that VP1 and VP2 were translated from subgenomic RNA using protein-specific antibodies in COS7 cells transfected with $pHuNoV_{U201F}$ [167]. The authors noted that antibodies raised against VP1, VP2, or whole VLPs derived from the serum of rabbits and guinea pigs were not able to detect this protein, suggesting either a translational inefficiency or structural variance of protein translated in this system [167]. Nevertheless, virus assembly was detected, and intact virions containing infectious RNA were observed in culture supernatant following CsCl gradient centrifugation [167]. The authors attempted to probe the reason for failure to detect VP1 expression by western blotting by substituting the gene for GFP into the virus ORF2, thereby preventing virus replication (as the virus cannot produce its capsid) yet allowing visualization of ORF2 translation [167]. GFP was detected at moderately low frequency in the transfected cells in a manner dependent on virus expression of VPg, as measured by immunofluorescence [167].

The translational inefficiencies in these published models offer an opportunity for significant improvement of virus protein expression. Even modest improvements in virus protein expression would greatly benefit these published rescue systems and facilitate study of HuNoV derived *de novo* from cDNA, as all rescue steps stem from the initial polyprotein translation and expression [12]. In order to increase protein expression in these systems, I decided to pursue three avenues thought to encourage RNA fidelity, longevity, and translatability: a 5’ Hammerhead ribozyme sequence, a longer poly-A tail length, and human codon optimization of the viral coding sequence [169].

The hammerhead ribozyme is an RNA motif that autocatalytically cleaves immediately downstream of itself to produce a blunt end to the RNA [170, 171]. This motif, named for its appearance similar to the head of a hammerhead shark, has been utilized in a rescue system for respiratory syncytial virus to produce an exact 5’ end to viral RNA [169]. Such an exact end is beneficial to the recovery of Norovirus as well as RSV, as exogenous nucleotides added by imprecise transcription initiation following the T7 or other promoter regions may interfere with the highly conserved UTR at the 5’ end of the viral genomic RNA [14-16, 169]. In the Asanaka report utilizing T7 promoter, only a few additional nucleotides were added to the 5’ end of the virus, but the 2014 Katayama report features an additional 107 exogenous nucleotides added to the 5’ end of the transcribed RNA, an addition that may reduce translatability of the viral RNA [19, 166]. I hypothesized that addition of a 5’ hammerhead ribozyme sequence to the viral

RNA would increase RNA fidelity to the native vRNA, thereby increasing viral protein expression and improving rescue efficiency.

HuNoV RNA is polyadenylated at the 3' end as a protection against cellular degradation [12]. The poly-A tail of mRNA in eukaryotic cells is slowly shortened over time as a mechanism for limiting protein expression, and non-adenylated RNA transcripts are quickly enzymatically degraded in the cytosol [18]. Increasing the length of the poly-A tail delays this shortening and thus degradation by cellular enzymes, which permits longer persistence of viral RNA. Longer-lived vRNA may in turn allow increased translation of viral protein. The systems for HuNoV rescue published to-date have utilized poly-A tracts encoded by the transfected cDNA to confer a poly-A tail of 26-30 nt to the transcribed viral RNA [19, 166]. Reports vary for the native length of HuNoV poly-A tails, but published values of 34-150 nucleotides suggests that the poly-A tail length in the published HuNoV rescue systems is too short [18, 19, 166]. I hypothesized that increasing the length of the poly-A tail to approximately 110 adenosine residues would increase RNA stability and permit translation of viral protein for longer duration, thereby increasing protein expression efficiency compared to constructs with shorter $A_{26\text{-}30}$ tails.

The final modification intended to increase viral protein expression involves the use of codon usage preference, or codon bias. Amino acids may be encoded through multiple redundant codons within the genome of a given organism. These codons may not be used at identical frequencies within a genome, and the collective frequency of codon usage is referred to as the codon bias for an organism. This bias confers fine control of protein expression because translation of protein from RNA is dependent on the availability of tRNA molecules for a given codon [172]. Codons with more abundant tRNA molecules are translated at higher efficiency than those with more scarce tRNA molecules. By adjusting the frequency of codon selection within an organism, translation may be modulated to increase or decrease efficiency by matching or avoiding the preferred codons; these processes are known as codon optimization or codon deoptimization, respectively [169, 172]. Human Norovirus shares the most common codon for a given amino acid with the human genome around 50% of the time, varying slightly by strain. By increasing codon usage concordance between the virus genome and the human genome, i.e. optimizing the virus for human expression, virus protein expression will increase in human cells based on the availability of tRNA molecules. This process has been utilized in helper plasmids for a rescue system for RSV, resulting in a nearly 100-fold increase of protein activity in a luciferase reporter assay, likely as a result of increased protein expression [169]. I hypothesized that adjusting the codon usage bias of the coding domains of human Norovirus to match the human codon usage bias while retaining known or predicted secondary RNA structures would increase Norovirus protein expression compared to wild-type Norovirus.

The overall goal of this project was to adapt the published systems for HuNoV rescue to the clinically relevant GII.4 strain. The overarching hypothesis of this project was that adding a 5' ribozyme sequence, increasing poly-A tail length, and adjusting the codon bias of HuNoV to match the most frequently used human codons while retaining known secondary structures would increase protein expression of HuNoV compared to the

published models for virus rescue. Furthermore, I hypothesized that increased protein expression would improve the rescue system for HuNoV, an improvement that would aid in study of this pathogen that plays an important role in diarrheal disease worldwide.

Experimental Approach

At the outset of this study, I elected to use the most recent GII.4 isolate with full genomic sequence data available in GenBank. I selected the GII.4 New Orleans isolate (GenBank accession JN595867.1), the primary cause of the 2010 U.S. outbreak, as the basis for the recovery system because full sequences of the emerging GII.4 Sydney isolate were not yet published [173]. This full genomic sequence is based on a clinical isolate taken from the stool of a symptomatic patient in May of 2010 and sequenced by Vega, et al. [173]. Nucleotide #4340, located in the viral polymerase, was altered in a silent mutation to give rise to a *NotI/EagI* restriction site in the construct design. This site was chosen to permit complete assembly from these two fragments and to permit modular replacement of various genome features (**Fig. 1**).

This genome construct was preceded on its 5' end by a *BstBI* restriction site to permit cloning into the bacterial artificial chromosome (BAC) vector pKBS6. This vector was adapted from pKBS5 through addition of a *NotI* sequence to the multiple cloning site, and was chosen for its stability even with large inserts, as well as the absence of translation in transformed bacteria, which limits cytotoxicity [169]. Following the *BstBI* sequence was a phi 10 T7 promoter sequence to drive transcription of the RNA in a T7-polymerase dependent manner [174]. A GGG spacer and an additional AAG motif followed this promoter. This AAG motif serves as 3 bases cleaved from the 5' end of the nascent transcript (AAG was chosen rather than AAA to eliminate a *MluI* restriction site). This sequence is followed by the hammerhead ribozyme sequence immediately upstream of the 5' end of the viral genome [171]. The genomic cDNA spans the next 7559 nucleotides of the construct and is followed by a poly-A tract of 110 adenosine residues followed immediately by a HDV ribozyme sequence designed to cut directly upstream of itself once transcribed, thus giving rise to a blunt 3' end of the poly-A tract at the tail of the viral RNA. This ribozyme was followed by a T7 terminator sequence and finished in an *MluI* restriction site to facilitate cloning into pKBS6. I assembled this construct in two steps by cloning the *BstBI-NotI* fragment into pKBS6 (pKBS6-HuNoV-A) and cloning the *NotI-MluI* fragment into the pKBS6-HuNoV-A construct to give rise to a BAC encoding full-length GII.4 2010 New Orleans HuNoV (pKBS6-HuNoV) (**Fig. 1**).

A second construct was assembled to probe the effect of human codon optimization on virus protein expression and rescue efficiency (**Fig. 2**). This construct, termed pKBS6-hOpt-HuNoV, was derived from the same GII.4 New Orleans HuNoV genotype as before (GenBank accession JN595867.1). This sequence was adapted and synthesized by Life Technologies's *GeneArt* service using a proprietary method to optimize the non-overlapping coding regions of ORFs 1-3 for human expression while retaining predicted RNA secondary structures. Junctions between the ORFs were not altered in order to preserve overlapping coding sequences, and a *NotI* restriction site was again added in the Pol segment of the ORF1 gene to permit virus assembly. All

other features of the construct, including ribozyme sequences and poly-A tract, were retained in this construct labeled pKBS6-hOpt-HuNoV (**Fig. 2**).

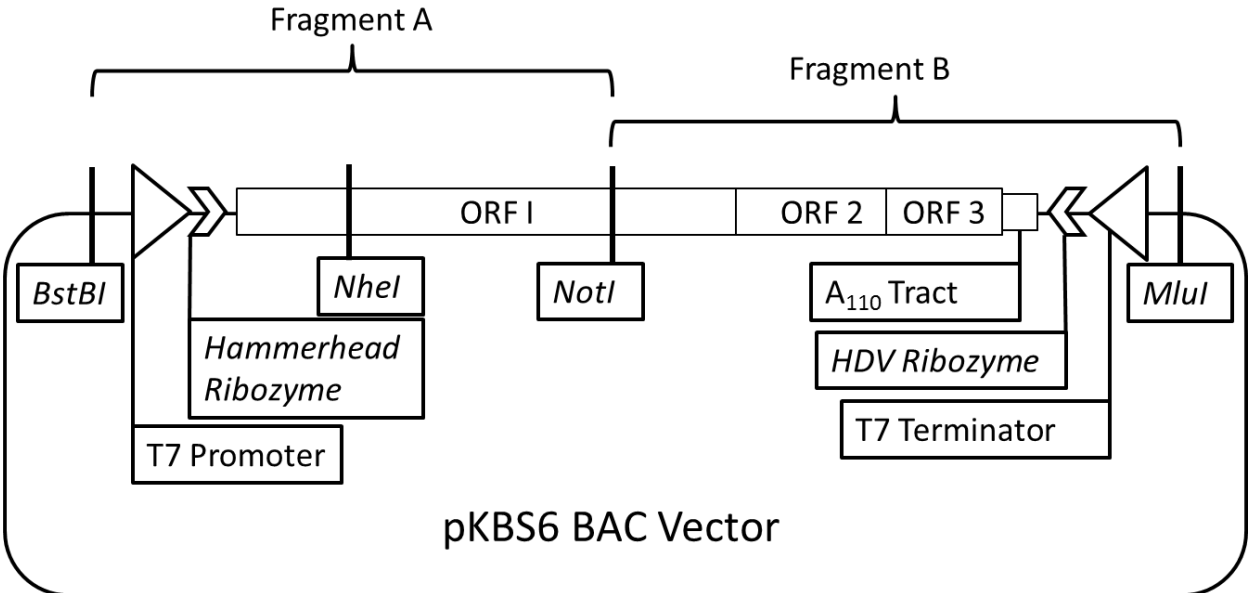

Figure 1: Design for construct to rescue GII.4 New Orleans HuNoV. A modular DNA clone encoding GII.4 New Orleans Norovirus (HuNoV) was synthesized and cloned into the pKBS6 bacterial artificial chromosome with T7 promoter, hammerhead ribozyme, A_{110} tract, HDV ribozyme, and T7 terminator sequences (pKBS6-HuNoV).

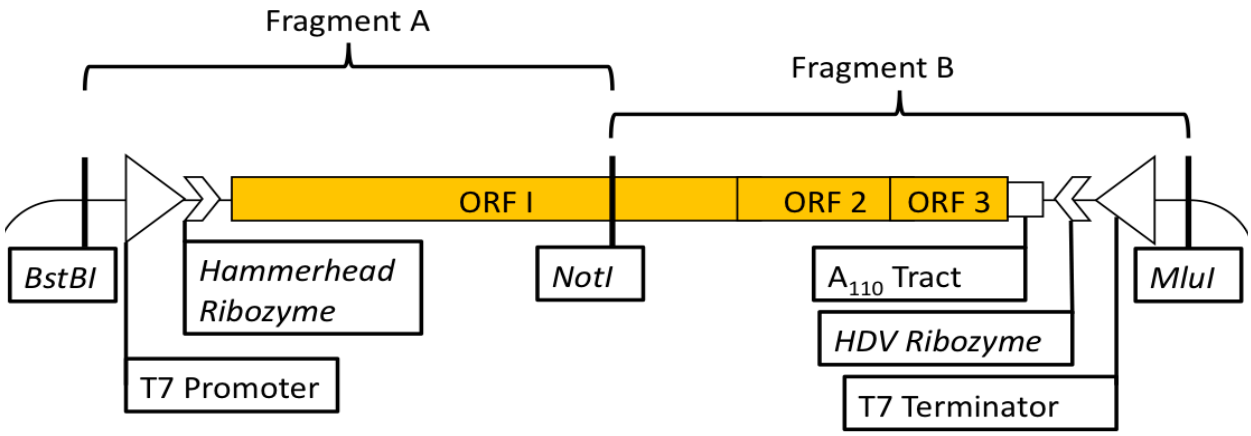

Figure 2. Alternative construct for probing the effect of virus codon optimization on translation efficacy and virus life cycle. A modular construct was created utilizing the indicated restriction sites. All coding regions of ORFs 1, 2, and 3 were optimized to match the most-commonly used human codon bias while preserving known RNA secondary structures (pKBS6-hOpt-HuNoV). Overlapping coding sequences at the ORF junctures were not altered in order to preserve both coding frames. Yellow indicates optimized region excluding ORF overlap.

DNA sequences were verified via restriction fragment length polymorphism analysis (**Fig. 3**). In short, assembled clones were digested using *HindIII* restriction enzyme (pKBS6-HuNoV) or *EcoRI* restriction enzyme (pKBS6-hOpt-HuNoV). Resultant digested DNA was resolved in a 100 mL 1% agarose in TAE gel for 1 hour, followed by 15 minutes staining in 5 μl/300 mL ethidium bromide in water and a 10 minute destain in 300 mL water. For pKBS6-HuNoV, both clones displayed match the predicted pattern of fragments at 10382, 2658, and 1331bp (**Fig. 3**). For pKBS6-hOpt-HuNoV, clone #3 displayed matched banding pattern of 8516, 4212, and 1664bp (**Fig. 3**). Glycerol stocks of these clones were prepared, and were used as DNA stock for all subsequent experiments.

Once the DNA sequence had been verified by RFLP analysis, the construct functionality was assessed by an in vitro transcription reaction to determine if RNA of correct length was produced from template DNA in a T7 polymerase-dependent manner (**Fig. 4**). Template DNA was linearized using an *MluI* site downstream of the assembled construct pKBS6-HuNoV. Resulting linear DNA was used as a template strand in the T7 Megascript *in vitro* transcription kit per manufacturer's protocol. Following the one-step incubation at 37ºC for 2 hours, the DNA and RNA mixture was treated with and without DNAse to confirm the presence of RNA. Following DNAse treatment, samples were resolved in a 1% agarose, 2.78% formaldehyde gel in MOPS buffer for one hour at 100 volts. Gel was visualized on a Chemidoc XRS gel document camera. RNA was detected only in lanes with RNA polymerase and a DNA template (**Fig. 4**). A faint band corresponding to linearized template DNA was detected in the control lane. DNAse treatment of the RNA slightly degraded the size of the RNA, suggesting either nonspecific nuclease activity of the DNAse or DNA fragments binding the RNA resulting in an electromobility shift. This RNA gel demonstrates that RNA of correct length is produced in an *in vitro* transcription reaction using T7 polymerase to transcribe the pKBS6-HuNoV cDNA construct.

Following *in vitro* verification of the ability of the construct to produce RNA of the correct length, either the DNA constructs or RNA transcribed *in vitro* from the DNA template were transfected into a baby hamster kidney cell line derivative (BSR.T7/5) or 293T cells stably transfected with a plasmid encoding T7 polymerase (293T.T7). The BSR cell line has been successfully utilized to recover infectious virus under control of a T7 promoter in a reverse genetics system for respiratory syncytial virus (RSV) described by the Moore lab and others [169]. Transfection was performed using 1μg of DNA or RNA and 1.6μl Lipofectamine 2000 reagent according to the manufacturer's protocol. Sixteen hours following transfection, transfection media was removed from the cells and replaced with standard growth media. Forty-eight hours following transfection, total RNA was isolated from the cells using Trizol reagent (Life Technologies) according to manufacturer's protocol. Growth media was aspirated from the cells and Trizol was added directly to the cells. Cells were lysed via vigorous pipetting before the addition of chloroform and phase separation via centrifugation at 12,000 x *g* for 15 minutes. RNA was isolated from the aqueous phase via isopropanol precipitation followed by centrifugation at 12,000 x *g* for 10 minutes at 4°C. Isolated RNA was treated both with and without DNAse to verify that RNA was not contaminated with DNA. A one-step

quantitative reverse transcriptase polymerase chain reaction (RT-PCR) was carried out on DNAse treated and untreated RNA using GII.4 detection probes (Cog2F: 5'-AAGAGCCAATGTTCAGATGG-3′ and Cog2R: 5′-CATTCACAAAACTGGGAGCC-3′) as well as a FAM-MGB probe with dual quenchers (Cog2P: 5'-/56-FAM/AGATCTGAG/Zen/CACGTGGGAGGG/3IABkFQ/-3′) [175]. DNA was quantified as relative fold expression compared to the input concentration of DNA prepared from bacterial culture (**Fig. 5)**. In no cases was RNA detected at greater relative expression compared to input DNA, suggesting that no RNA replication had occurred. Both input and maxiprep DNA were significantly degraded by DNAse, while RNA concentrations were not significantly changed in the presence of DNAse.

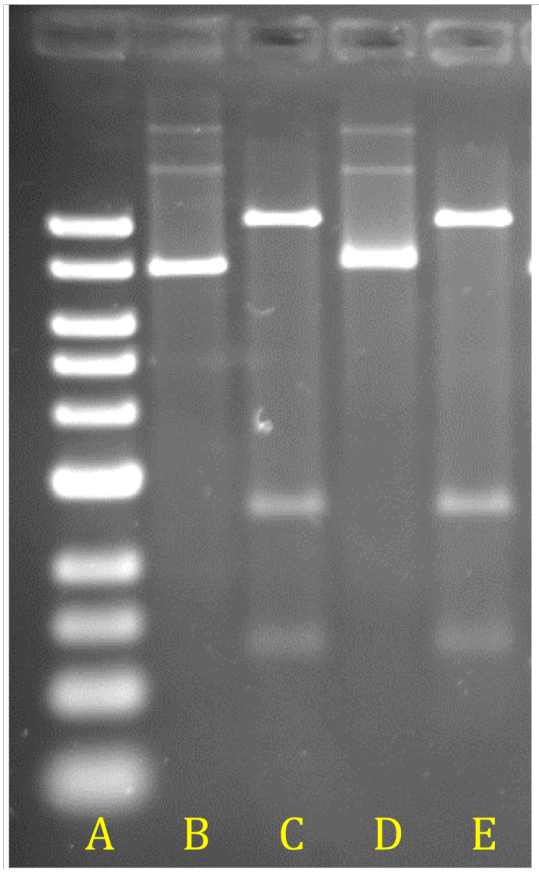

Lane A) 1kb DNA ladder
Lane B) Uncut pKBS6-HuNoV #1
Lane C) *HindIII*-cut pKBS6-HuNoV #1
Lane D) Uncut pKBS6-HuNoV #2
Lane E) *HindIII*-cut pKBS6-HuNoV #2

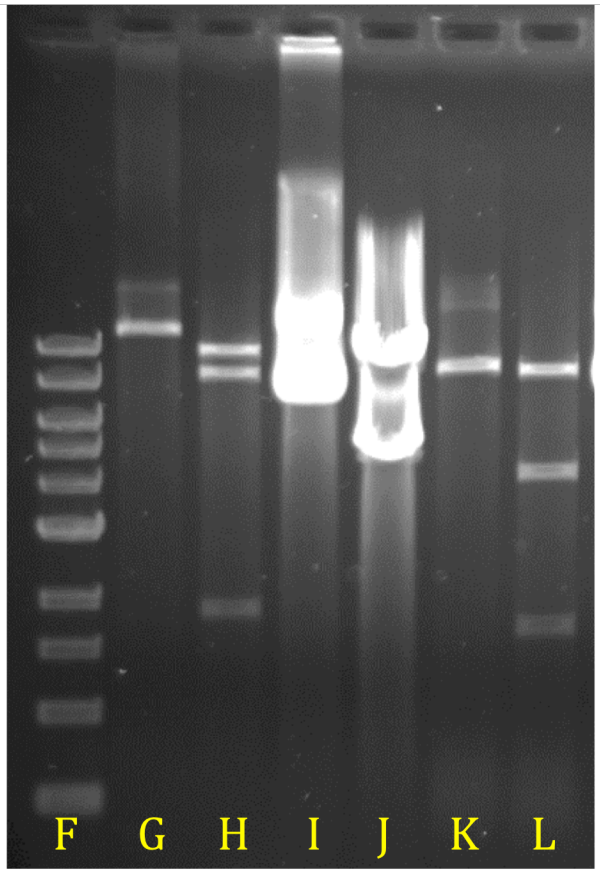

Lane F) 1kb DNA ladder
Lane G) Uncut pKBS6-hOpt-HuNoV #1
Lane H) *EcoRI*-cut pKBS6-hOpt-HuNoV #1
Lane I) Uncut pKBS6-hOpt-HuNoV #2
Lane J) *EcoRI* -cut pKBS6-hOpt-HuNoV #2
Lane K) Uncut pKBS6-hOpt-HuNoV #3
Lane L) *EcoRI* -cut pKBS6-hOpt-HuNoV #3

Figure 3. RFLP analysis of pKBS6-HuNoV and pKBS6-hOpt-HuNoV. Clones of *E. coli* were transformed with constructs encoding wild-type and human optimized HuNoV. DNA prepared from the bacteria was cut with *HindIII* or *EcoRI* restriction enzymes for 1 hour followed by gel electrophoresis. Predicted band sizes are 10382, 2658, and

1331bp for WT pKBS6-HuNoV, indicating valid construct assembly in both clones shown. Predicted band sizes are 8516, 4212, and 1664bp for pKBS6-hOpt-HuNoV, indicating valid construct assembly in clone #3.

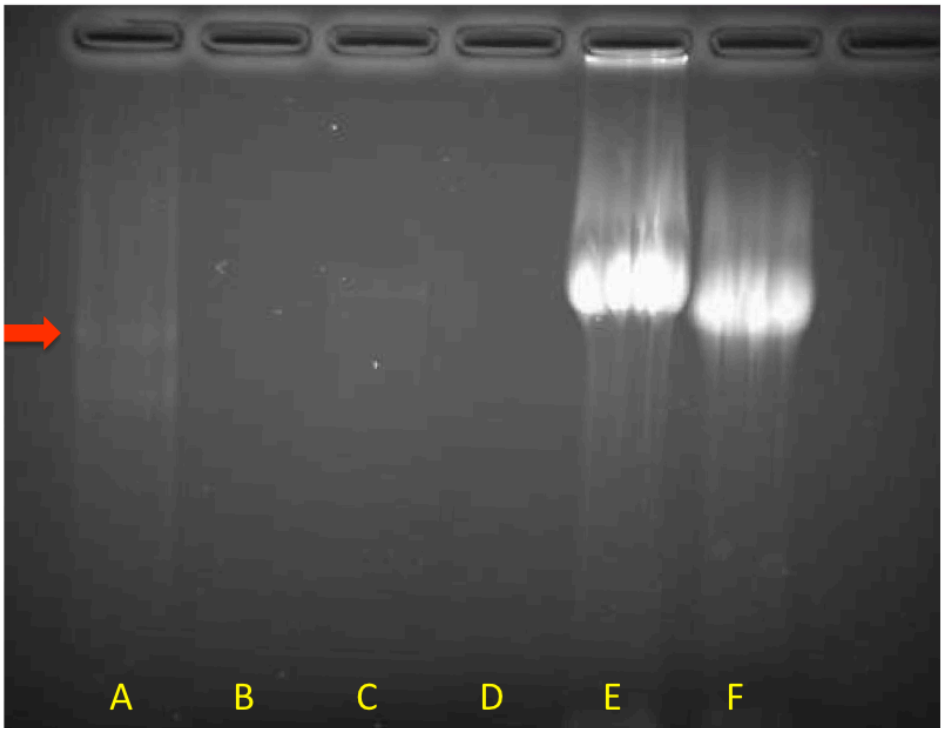

Lane A) Dig-labeled RNA Marker I
Lane B) Water control
Lane C) Input DNA
Lane D) Input DNA + DNAse
Lane E) RNA Transcript
Lane F) RNA Transcript + DNAse

Figure 4: *In vitro* transcription of pKBS6-HuNoV yields RNA of correct length. RNA was transcribed from the base HuNoV construct to yield transcripts of predicted length 7669bp. Red arrow denotes top ladder band at 6948bp. DNAse treatment of RNA caused an electromobility shift, suggesting either DNA contamination or imprecise enzyme activity.

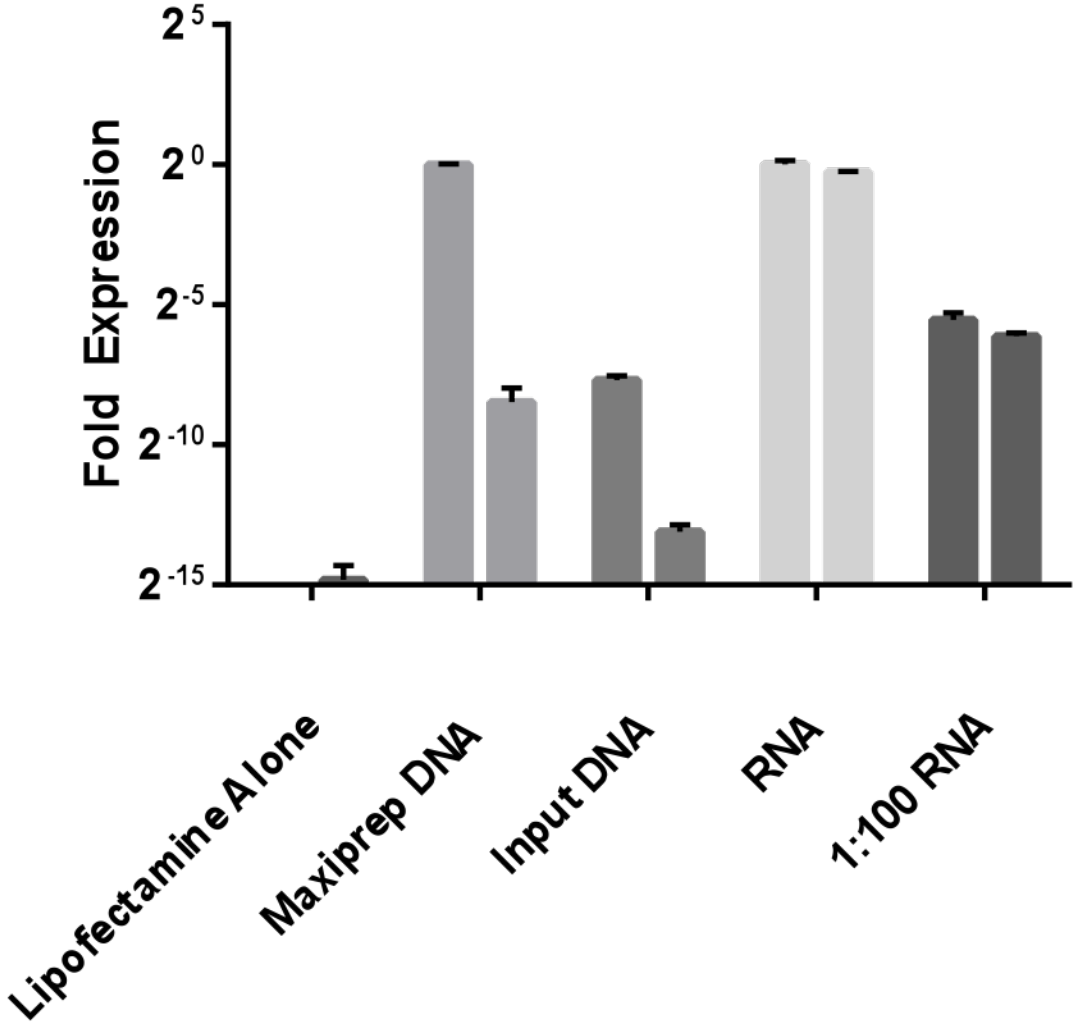

Figure 5: Norovirus RNA is detectable in transfected cells 48h post transfection. BSR.T7/5 cells were transfected with 1μg DNA or RNA using 1.6μl Lipofectamine 2000. After 48 hours, cells were washed with phosphate-buffered saline (PBS) and then extracted using Trizol reagent. RNA was eluted using isopropanol precipitation and qRT-PCR was performed on RNA using Cog2 primers following treatment with and without DNAse. Relative expression compared to transfected maxiprep Norovirus DNA construct is shown. n=2 wells/group.

I next assayed for viral major capsid protein VP1 expression as a marker for progression through the virus life cycle. BSR.T7/5 cells transfected with the pKBS6-HuNoV and pKBS6-hOpt-HuNoV constructs were permitted to grow for four days. No obvious cytopathic effects (CPE) were observed in any transfection condition, an observation consistent with the fact that HuNoV does not grossly disrupt the intestinal epithelial structure [83]. Ninety-six hours following transfection, growth media was removed from the cells, which were subsequently lysed through the direct addition of

radioimmunoprecipitation assay (RIPA) buffer with 1% protease inhibitor cocktail. Cells were lysed on ice for 10 minutes and then clarified by centrifugation at 13,000 rpm at 4°C. Supernatant was removed and mixed at 1:1 ratio with Laemmli sample buffer containing beta-mercaptoethanol. Resultant mixture was boiled at 95°C for 10 minutes and then chilled on ice before loading into a 10% sodium dodecyl sulfate – polyacrylamide gel electrophoresis (SDS-PAGE) gel and electrophoresed at 100 V for one hour. Protein was transferred from this gel to a polyvinylidene difluoride (PVDF) membrane at 100 V for 90 minutes. The membrane was blocked with 5% powdered milk in Tris-buffered saline with 0.05% Tween-20 (TBST) overnight at 4°C. Blot was then probed with polyclonal rabbit antibodies raised against GII.4 VLP rescued by baculovirus expression in Sf9 cells to detect GII.4 New Orleans VP1 protein expression. A VLP (GII.4 Grimsby strain) was used as a positive control. The antibody successfully bound the VLP positive control, but in no rescue condition was VP1 protein detected (**Fig. 6**). Additional antibodies for VLP and VP1 detection were used in other independent experiments and either did not detect VP1 in any condition or were nonspecific and detected protein in all lanes, including mock transfections. Equal loading was verified by stripping the blot and re-probing with a mouse monoclonal anti-GAPDH antibody (**Fig. 6**). In addition to BSR cells, 293T, Hep2, Vero, and HeLa cells were transfected; all showed a complete lack of VP1 expression.

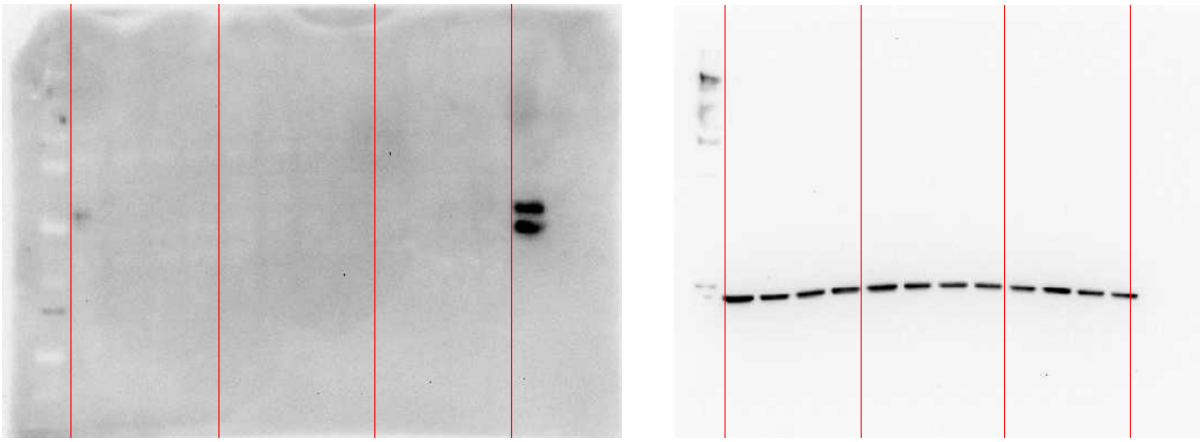

Figure 6: Norovirus VP1 protein is not expressed in transfected cells. BSR.T7/5 cells were transfected with uncapped (4 left lanes), capped (4 right lanes), or a 1:1 mix of capped and uncapped (4 center lanes) RNA encoding, from left to right, mock, WT Norovirus, hOpt Norovirus, and GFP. On the far right is a positive control GII.4 Grimsby VLP. Left blot was probed with rabbit polyclonal antibody raised against GII.4 Farmington Hills VLP. Right blot was probed with mouse monoclonal anti-GAPDH.

To determine the point of translational failure in the virus life cycle, new constructs were assembled utilizing a fluorescent reporter gene monomeric Katushka 2 inserted into the genome of GII.4 New Orleans HuNoV similar to a previously published approach (**Fig. 7**) [167]. In short, a segment of the virus genome spanning a portion of the nonstructural protein coding ORF1 between the naturally occurring unique

restriction sites *NheI* and *NotI* was synthesized with the gene for mKate2 inserted between the p41 and p22 genes, yielding the construct dubbed pKBS6-K-HuNoV (**Fig. 7**). This gene was flanked with QG dipeptides to serve as substrates for the viral protease, which would cleave and liberate the translated fluorescent protein, which is active as a monomer and thus fluoresces red without additional modification.

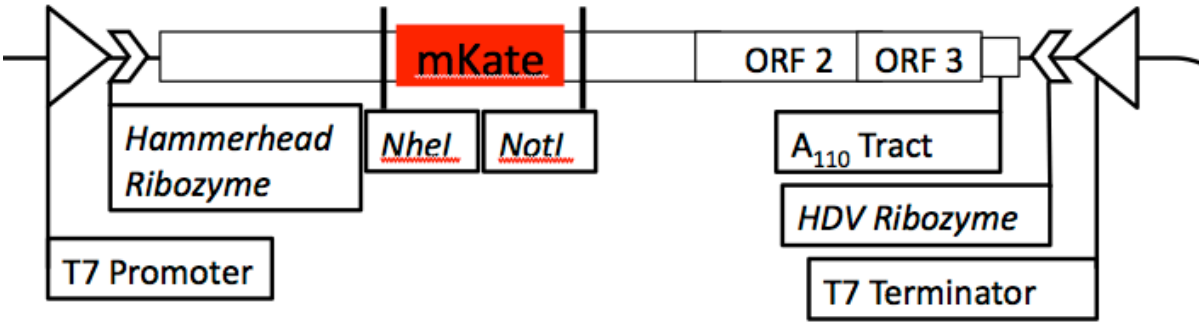

Figure 7. Fluorescent reporter construct for probing the translation of ORF1. A modular construct was created utilizing the indicated restriction sites. The gene for monomeric Katushka 2 protein was inserted between the p41 (NTPase) and p22 (3A-like) gene regions, flanked by the FELQG substrate sites for the viral protease.

This fluorescent reporter construct was transfected into either BSR.T7/5 or HEK293T cells. Cells were assayed daily for fluorescence following transfection with these constructs or with a previously published construct encoding a GFP-tagged HuNoV [167]. Fluorescence was not detected in any of the GII.4 constructs from days 0 to 4 post-transfection, while the control GII.3 constructs, a GFP plasmid under control of a T7 promoter, and another unrelated fluorescently tagged virus RSV all demonstrated fluorescence by days 1-2 that persisted until day 4 (**Fig. 8**). Fluorescence in the GII.3 virus was substantially reduced compared to other transfection controls, again highlighting the extremely low translational efficiency in the published system. CPE was detected in portions of the GFP labeled Norovirus transfection control only, in contrast to previous reports of limited CPE. Fluorescence induced by transfection with RSV constructs was rare, but robust in those cells successfully transfected.

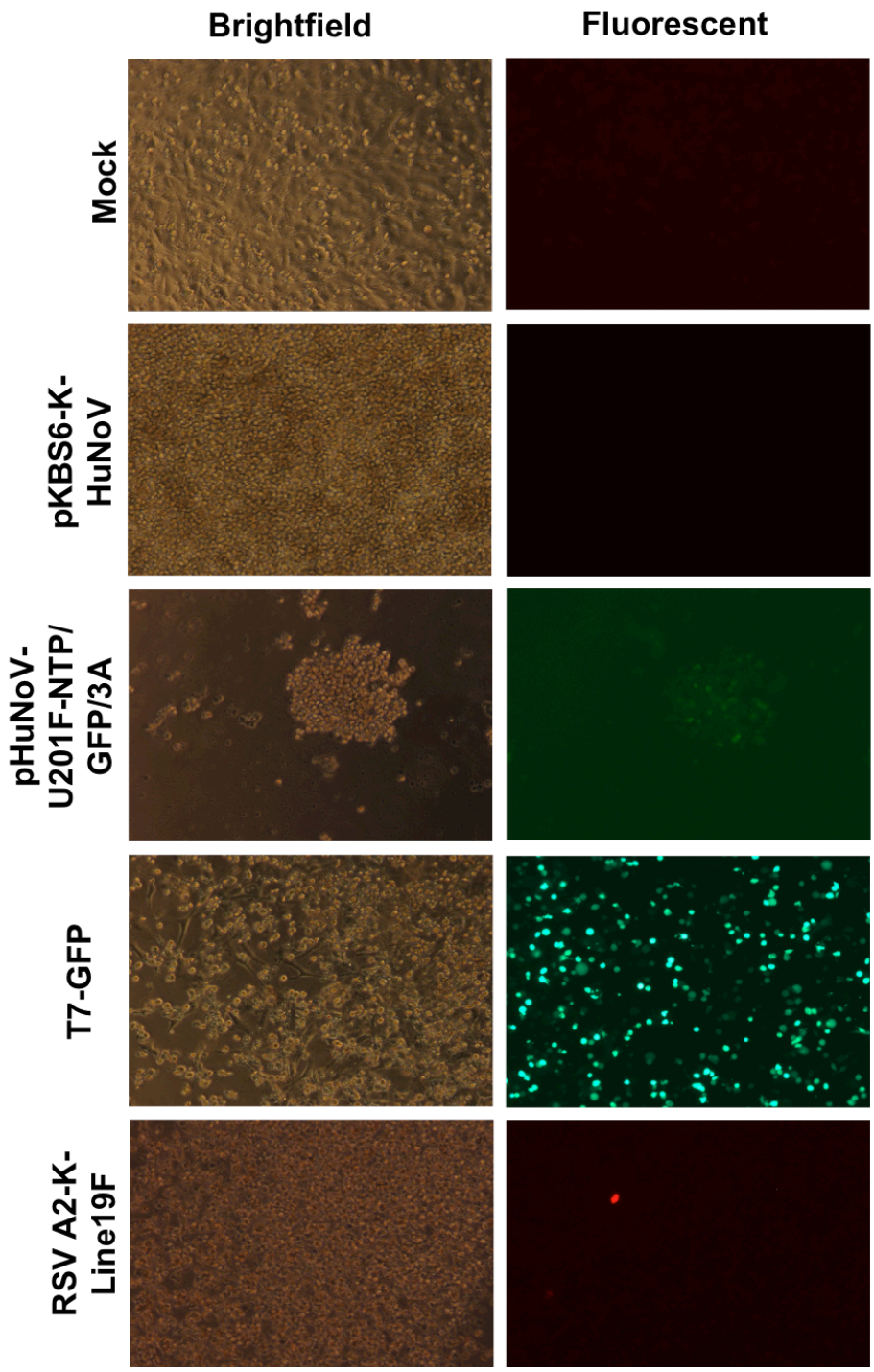

Figure 8: Fluorescence is not detected in BSR.T7/5 cells transfected with pKBS6-K-HuNoV. DNA constructs were assembled and validated by RFLP before transfection into BSR.T7/5 cells. Cells were examined daily by fluorescent microscopy for four days to detect fluorescent reporter protein expression. Images shown were brightened by 30% in Axiovision with the exception of the T7-GFP fluorescent and the RSV fluorescent images. No red fluorescence was detected in the Katushka labeled pKBS6-K-HuNoV. Extremely low fluorescence was detected in the pHunOV-U201F-NTP/GFP/3A control plasmid when compared to the T7-GFP transfection control. Red fluorescence was detected in RSV-transfected controls.

Conclusions

Constructs encoding both wild-type and human optimized GII.4 New Orleans HuNoV were synthesized and assembled via restriction digest and ligation. Sequences of these constructs were verified via RFLP analysis and *in vitro* transcription using a T7 polymerase-based system produced RNA of the appropriate length corresponding to genomic viral RNA. Furthermore, when these DNA constructs or RNA transcribed *in vitro* from these constructs was transfected into cells encoding T7-polymerase, RNA was detectable in cells up to 72 hours post-transfection. This RNA did not give rise to measurable expression of VP1, a protein produced late in the virus life cycle, in 293T or BSR.T7/5 cells. New constructs were assembled to probe early viral protein expression through the addition of a monomeric fluorescent reporter gene to ORF1 of the viral genome. Transfection of this new GII.4 did not yield fluorescent signal in contrast to previously published fluorescently labeled GII.3 virus, suggesting a fundamental difference between these two virus genotypes that is not limited to the ORF2 major capsid protein VP1. Fluorescence of the control GII.3 virus was low compared to standard transfection controls, confirming the low protein expression in the previously published rescue model in 293T cells.

This finding has re-emphasized the need for a robust rescue system of GII.4 HuNoV, as differences between viral strains cannot be easily studied using the currently published systems. Improvements to the virus rescue system rely on a more thorough understanding of virus biology and strain differences. As a result, progress in understanding the biology of human Norovirus is likely to continue to lag compared to more rescuable and cultivatable viruses.

Chapter 3 – Summary and Future Directions

In this thesis I have described my attempts at adapting the published rescue systems for GI.1 and GII.3 human Norovirus to the clinically relevant GII.4 HuNoV strain, as well as attempts to increase viral protein expression by adding a 5' hammerhead ribozyme sequence, elongating the poly-A tail from the published 26-30 adenosine residues to the more physiological 110 residues, and optimizing the HuNoV genome for human protein expression. Viral protein expression was found to be independent of the 5' ribozyme, increased poly-A tail length, and human codon optimization, and no virus was detected in this rescue system by RT-PCR for viral genome replication or western blotting for VP1 capsid protein expression. In an attempt to probe the limiting step of the GII.4 life cycle, a novel construct encoding a virus with the exogenous fluorescent reporter mKate2 was assembled and transfected into cells in an adaptation of a previously published rescue protocol. This fluorescent construct did not give rise to fluorescent protein expression in either of the cell lines or in any of the GII.4 virus constructs tested, contrasting with weak fluorescent protein expressed in the GII.3 control. The complete lack of fluorescent protein expression indicates that the pioneer round of viral translation documented in GII.3 Norovirus is not occurring in GII.4 Norovirus encoded by the pKBS6-HuNoV construct. These findings suggest a novel and fundamental difference in the life cycle between the viruses recovered in previous rescue systems and the clinically relevant GII.4 strain.

The lack of fluorescent reporter protein expression following transfection suggests that viral protein translation is not initiating from the pKBS6-HuNoV construct. The requirements for VPg conjugation, while incompletely understood for HuNoV, have been demonstrated for other members of *Caliciviridae*. In the constructs tested in this thesis, VPg may be unable to bind to the RNA following ribozyme cleavage due to the normal process of VPg uridilylation by the viral RdRP. This process may be strain-dependent, and GII.4 virus may rely more on VPg than other strains to initiate transcription and translation. A future approach to test this hypothesis would be to chemically conjugate the VPg to viral RNA *in vitro* prior to transfection to assay the effect of VPg on RNA stability and thus protein expression. An alternate approach would be to supply VPg and Pol *in trans*, an approach currently under investigation in our lab.

The failure of this construct to rescue GII.4 HuNoV may reflect an incompatibility between the virus and the cell lines used in the transfections. BSR.T7/5 cells have been successfully utilized in other rescue systems, but these cells may not meet the as yet undefined conditions for support of viral replication. The lack of GII.4 viral fluorescent protein expression in transfected 293T cells compared to the fluorescent reporter GII.3 virus suggests that while 293T cells may support viral replication for GII.3, they are not permissive to GII.4 replication. This observation suggests that a fundamental difference exists between GII.3 and GII.4 virus, a hypothesis that merits additional study, as no reports exist detailing life cycle differences between the various genotypes of HuNoV.

In other models of virus rescue, low initial rescue efficiency is less important than in Norovirus due to subsequent ability to expand rescued virus in permissive cells. As Norovirus is difficult to grow *in vitro*, this low initial rescue efficiency cannot be

compensated by subsequent culture. The recent discovery that enteric bacteria support HuNoV infection and replication in human B cells offers one potential approach to increase viral titer following initial rescue. This system also suggests that Norovirus may have other requirements for viral infection of host cells compared to currently rescuable viruses. One future experiment would be to attempt rescue of the virus utilizing eIF1α or similar promoter sequence in the BJAB cells known to be permissive to viral replication. Alternatively, co-culture of transfected cells with enteric bacteria might aid in virus rescue.

Human Norovirus continues to pose a significant health burden worldwide. The research described in this thesis demonstrates that our understanding of virus biology, including genome expression and life cycle progression, is incomplete. Continued studies utilizing the new breakthroughs in the field for culturing virus, as well as continued efforts to improve upon the published rescue systems, will further our knowledge of how to address this important cause of diarrheal disease.

References:

1. J, Z., *Hyperemesis Hiemis or the Winter Vomiting Disease.* Arch. Pediat., 1929. **46**: p. 391.
2. Kapikian, A.Z., et al., *Visualization by immune electron microscopy of a 27-nm particle associated with acute infectious nonbacterial gastroenteritis.* J Virol, 1972. **10**(5): p. 1075-81.
3. Dolin, R., et al., *Transmission of acute infectious nonbacterial gastroenteritis to volunteers by oral administration of stool filtrates.* J Infect Dis, 1971. **123**(3): p. 307-12.
4. *Virus Taxonomy: 1995 Release*, in *ICTV 6th Report (MSL #14)*. 1995, International Committee on Taxonomy of Viruses.
5. *Caliciviruses: Molecular and Cellular Virology*, ed. G. Hansman. 2010: Caister Academic Press.
6. *Virus Taxonomy: Classification and Nomenclature of Viruses*, ed. M.J.A. Andrew M.Q. King, Eric B. Carstens, Elliot J. Lefkowitz. Vol. 9. 2012, San Diego: Elsevier Academic Press.
7. Zheng, D.P., et al., *Norovirus classification and proposed strain nomenclature.* Virology, 2006. **346**(2): p. 312-23.
8. Jiang, X., et al., *Detection of Norwalk virus in stool by polymerase chain reaction.* J Clin Microbiol, 1992. **30**(10): p. 2529-34.
9. Okada, M., et al., *Genetic analysis of noroviruses in Chiba Prefecture, Japan, between 1999 and 2004.* J Clin Microbiol, 2005. **43**(9): p. 4391-401.
10. *Emergence of new norovirus strain GII.4 Sydney--United States, 2012.* MMWR Morb Mortal Wkly Rep, 2013. **62**(3): p. 55.
11. Prevention, C.f.D.C.a. *Norovirus*. 2015 [cited 2015 04/13/2015]; Available from: http://www.cdc.gov/norovirus/.
12. Thorne, L.G. and I.G. Goodfellow, *Norovirus gene expression and replication.* J Gen Virol, 2014. **95**(Pt 2): p. 278-91.
13. Gutierrez-Escolano, A.L., et al., *Interaction of cellular proteins with the 5′ end of Norwalk virus genomic RNA.* J Virol, 2000. **74**(18): p. 8558-62.
14. Bailey, D., et al., *Functional analysis of RNA structures present at the 3′ extremity of the murine norovirus genome: the variable polypyrimidine tract plays a role in viral virulence.* J Virol, 2010. **84**(6): p. 2859-70.
15. McFadden, N., et al., *Norovirus regulation of the innate immune response and apoptosis occurs via the product of the alternative open reading frame 4.* PLoS Pathog, 2011. **7**(12): p. e1002413.
16. Simmonds, P., et al., *Bioinformatic and functional analysis of RNA secondary structure elements among different genera of human and animal caliciviruses.* Nucleic Acids Res, 2008. **36**(8): p. 2530-46.
17. Hardy, M.E., *Norovirus protein structure and function.* FEMS Microbiol Lett, 2005. **253**(1): p. 1-8.
18. Rohayem, J., et al., *Protein-primed and de novo initiation of RNA synthesis by norovirus 3Dpol.* J Virol, 2006. **80**(14): p. 7060-9.
19. Asanaka, M., et al., *Replication and packaging of Norwalk virus RNA in cultured mammalian cells.* Proc Natl Acad Sci U S A, 2005. **102**(29): p. 10327-32.

20. Fernandez-Vega, V., et al., *Norwalk virus N-terminal nonstructural protein is associated with disassembly of the Golgi complex in transfected cells.* J Virol, 2004. **78**(9): p. 4827-37.
21. Hughes, P.J. and G. Stanway, *The 2A proteins of three diverse picornaviruses are related to each other and to the H-rev107 family of proteins involved in the control of cell proliferation.* J Gen Virol, 2000. **81**(Pt 1): p. 201-7.
22. Ettayebi, K. and M.E. Hardy, *Norwalk virus nonstructural protein p48 forms a complex with the SNARE regulator VAP-A and prevents cell surface expression of vesicular stomatitis virus G protein.* J Virol, 2003. **77**(21): p. 11790-7.
23. Pfister, T. and E. Wimmer, *Polypeptide p41 of a Norwalk-like virus is a nucleic acid-independent nucleoside triphosphatase.* J Virol, 2001. **75**(4): p. 1611-9.
24. Green, K.Y., et al., *Isolation of enzymatically active replication complexes from feline calicivirus-infected cells.* J Virol, 2002. **76**(17): p. 8582-95.
25. Daughenbaugh, K.F., et al., *The genome-linked protein VPg of the Norwalk virus binds eIF3, suggesting its role in translation initiation complex recruitment.* Embo j, 2003. **22**(11): p. 2852-9.
26. Sosnovtsev, S. and K.Y. Green, *RNA transcripts derived from a cloned full-length copy of the feline calicivirus genome do not require VpG for infectivity.* Virology, 1995. **210**(2): p. 383-90.
27. Herbert, T.P., I. Brierley, and T.D. Brown, *Identification of a protein linked to the genomic and subgenomic mRNAs of feline calicivirus and its role in translation.* J Gen Virol, 1997. **78 (Pt 5)**: p. 1033-40.
28. Goodfellow, I., et al., *Calicivirus translation initiation requires an interaction between VPg and eIF 4 E.* EMBO Rep, 2005. **6**(10): p. 968-72.
29. Royall, E., et al., *Murine norovirus 1 (MNV1) replication induces translational control of the host by regulating eIF4E activity during infection.* J Biol Chem, 2015. **290**(8): p. 4748-58.
30. Chung, L., et al., *Norovirus translation requires an interaction between the C Terminus of the genome-linked viral protein VPg and eukaryotic translation initiation factor 4G.* J Biol Chem, 2014. **289**(31): p. 21738-50.
31. Machin, A., J.M. Martin Alonso, and F. Parra, *Identification of the amino acid residue involved in rabbit hemorrhagic disease virus VPg uridylylation.* J Biol Chem, 2001. **276**(30): p. 27787-92.
32. Belliot, G., et al., *Nucleotidylylation of the VPg protein of a human norovirus by its proteinase-polymerase precursor protein.* Virology, 2008. **374**(1): p. 33-49.
33. Liu, B., I.N. Clarke, and P.R. Lambden, *Polyprotein processing in Southampton virus: identification of 3C-like protease cleavage sites by in vitro mutagenesis.* J Virol, 1996. **70**(4): p. 2605-10.
34. Liu, B.L., et al., *Identification of further proteolytic cleavage sites in the Southampton calicivirus polyprotein by expression of the viral protease in E. coli.* J Gen Virol, 1999. **80 (Pt 2)**: p. 291-6.
35. Vazquez, A.L., et al., *Expression of enzymatically active rabbit hemorrhagic disease virus RNA-dependent RNA polymerase in Escherichia coli.* J Virol, 1998. **72**(4): p. 2999-3004.
36. Ng, K.K., et al., *Crystal structures of active and inactive conformations of a caliciviral RNA-dependent RNA polymerase.* J Biol Chem, 2002. **277**(2): p. 1381-7.

37. Ng, K.K., et al., *Crystal structure of norwalk virus polymerase reveals the carboxyl terminus in the active site cleft.* J Biol Chem, 2004. **279**(16): p. 16638-45.
38. Prasad, B.V., et al., *X-ray crystallographic structure of the Norwalk virus capsid.* Science, 1999. **286**(5438): p. 287-90.
39. Tan, M., et al., *Mutations within the P2 domain of norovirus capsid affect binding to human histo-blood group antigens: evidence for a binding pocket.* J Virol, 2003. **77**(23): p. 12562-71.
40. Prasad, B.V., et al., *Three-dimensional structure of baculovirus-expressed Norwalk virus capsids.* J Virol, 1994. **68**(8): p. 5117-25.
41. Jiang, X., et al., *Expression, self-assembly, and antigenicity of the Norwalk virus capsid protein.* J Virol, 1992. **66**(11): p. 6527-32.
42. Treanor, J.J., et al., *A novel intramuscular bivalent norovirus virus-like particle vaccine candidate--reactogenicity, safety, and immunogenicity in a phase 1 trial in healthy adults.* J Infect Dis, 2014. **210**(11): p. 1763-71.
43. Wirblich, C., H.J. Thiel, and G. Meyers, *Genetic map of the calicivirus rabbit hemorrhagic disease virus as deduced from in vitro translation studies.* J Virol, 1996. **70**(11): p. 7974-83.
44. Sosnovtsev, S.V. and K.Y. Green, *Identification and genomic mapping of the ORF3 and VPg proteins in feline calicivirus virions.* Virology, 2000. **277**(1): p. 193-203.
45. Glass, P.J., et al., *Norwalk virus open reading frame 3 encodes a minor structural protein.* J Virol, 2000. **74**(14): p. 6581-91.
46. Winkler, F.K., et al., *Tomato bushy stunt virus at 5.5-A resolution.* Nature, 1977. **265**(5594): p. 509-13.
47. Sosnovtsev, S.V., et al., *Feline calicivirus VP2 is essential for the production of infectious virions.* J Virol, 2005. **79**(7): p. 4012-24.
48. Jones, M.K., et al., *Enteric bacteria promote human and mouse norovirus infection of B cells.* Science, 2014. **346**(6210): p. 755-9.
49. Singh, B.K., M.M. Leuthold, and G.S. Hansman, *Human noroviruses' fondness for histo-blood group antigens.* J Virol, 2015. **89**(4): p. 2024-40.
50. Makino, A., et al., *Junctional adhesion molecule 1 is a functional receptor for feline calicivirus.* J Virol, 2006. **80**(9): p. 4482-90.
51. Ossiboff, R.J., et al., *Conformational changes in the capsid of a calicivirus upon interaction with its functional receptor.* J Virol, 2010. **84**(11): p. 5550-64.
52. Stuart, A.D. and T.D. Brown, *Entry of feline calicivirus is dependent on clathrin-mediated endocytosis and acidification in endosomes.* J Virol, 2006. **80**(15): p. 7500-9.
53. Kreutz, L.C. and B.S. Seal, *The pathway of feline calicivirus entry.* Virus Res, 1995. **35**(1): p. 63-70.
54. Shivanna, V., Y. Kim, and K.O. Chang, *The crucial role of bile acids in the entry of porcine enteric calicivirus.* Virology, 2014. **456-457**: p. 268-78.
55. Shivanna, V., Y. Kim, and K.O. Chang, *Endosomal acidification and cathepsin L activity is required for calicivirus replication.* Virology, 2014. **464-465**: p. 287-95.
56. Taube, S., et al., *Ganglioside-linked terminal sialic acid moieties on murine macrophages function as attachment receptors for murine noroviruses.* J Virol, 2009. **83**(9): p. 4092-101.

57. Gerondopoulos, A., et al., *Murine norovirus-1 cell entry is mediated through a non-clathrin-, non-caveolae-, dynamin- and cholesterol-dependent pathway.* J Gen Virol, 2010. **91**(Pt 6): p. 1428-38.
58. Belliot, G., et al., *In vitro proteolytic processing of the MD145 norovirus ORF1 nonstructural polyprotein yields stable precursors and products similar to those detected in calicivirus-infected cells.* J Virol, 2003. **77**(20): p. 10957-74.
59. Wobus, C.E., et al., *Replication of Norovirus in cell culture reveals a tropism for dendritic cells and macrophages.* PLoS Biol, 2004. **2**(12): p. e432.
60. Hyde, J.L. and J.M. Mackenzie, *Subcellular localization of the MNV-1 ORF1 proteins and their potential roles in the formation of the MNV-1 replication complex.* Virology, 2010. **406**(1): p. 138-48.
61. Subba-Reddy, C.V., et al., *Norovirus RNA synthesis is modulated by an interaction between the viral RNA-dependent RNA polymerase and the major capsid protein, VP1.* J Virol, 2012. **86**(18): p. 10138-49.
62. Liu, Y., E. Wimmer, and A.V. Paul, *Cis-acting RNA elements in human and animal plus-strand RNA viruses.* Biochim Biophys Acta, 2009. **1789**(9-10): p. 495-517.
63. Alonso, C., et al., *Programmed cell death in the pathogenesis of rabbit hemorrhagic disease.* Arch Virol, 1998. **143**(2): p. 321-32.
64. Bok, K., et al., *Apoptosis in murine norovirus-infected RAW264.7 cells is associated with downregulation of survivin.* J Virol, 2009. **83**(8): p. 3647-56.
65. Siebenga, J.J., et al., *Epochal evolution of GGII.4 norovirus capsid proteins from 1995 to 2006.* J Virol, 2007. **81**(18): p. 9932-41.
66. Koelle, K., et al., *Epochal evolution shapes the phylodynamics of interpandemic influenza A (H3N2) in humans.* Science, 2006. **314**(5807): p. 1898-903.
67. Nilsson, M., et al., *Evolution of human calicivirus RNA in vivo: accumulation of mutations in the protruding P2 domain of the capsid leads to structural changes and possibly a new phenotype.* J Virol, 2003. **77**(24): p. 13117-24.
68. Frenck, R., et al., *Predicting susceptibility to norovirus GII.4 by use of a challenge model involving humans.* J Infect Dis, 2012. **206**(9): p. 1386-93.
69. Bull, R.A., et al., *Rapid evolution of pandemic noroviruses of the GII.4 lineage.* PLoS Pathog, 2010. **6**(3): p. e1000831.
70. Kroneman, A., et al., *Analysis of integrated virological and epidemiological reports of norovirus outbreaks collected within the Foodborne Viruses in Europe network from 1 July 2001 to 30 June 2006.* J Clin Microbiol, 2008. **46**(9): p. 2959-65.
71. Shanker, S., et al., *Structural analysis of histo-blood group antigen binding specificity in a norovirus GII.4 epidemic variant: implications for epochal evolution.* J Virol, 2011. **85**(17): p. 8635-45.
72. Lindesmith, L.C., et al., *Emergence of a norovirus GII.4 strain correlates with changes in evolving blockade epitopes.* J Virol, 2013. **87**(5): p. 2803-13.
73. Glass, R.I., U.D. Parashar, and M.K. Estes, *Norovirus gastroenteritis.* N Engl J Med, 2009. **361**(18): p. 1776-85.
74. Abe, T., et al., *Infantile convulsions with mild gastroenteritis.* Brain Dev, 2000. **22**(5): p. 301-6.
75. Turcios-Ruiz, R.M., et al., *Outbreak of necrotizing enterocolitis caused by norovirus in a neonatal intensive care unit.* J Pediatr, 2008. **153**(3): p. 339-44.

76. Marshall, J.K., et al., *Postinfectious irritable bowel syndrome after a food-borne outbreak of acute gastroenteritis attributed to a viral pathogen.* Clin Gastroenterol Hepatol, 2007. **5**(4): p. 457-60.
77. Gebhard, R.L., et al., *Acute viral enteritis and exacerbations of inflammatory bowel disease.* Gastroenterology, 1982. **83**(6): p. 1207-9.
78. Mattner, F., et al., *Risk groups for clinical complications of norovirus infections: an outbreak investigation.* Clin Microbiol Infect, 2006. **12**(1): p. 69-74.
79. Frange, P., et al., *Prevalence and clinical impact of norovirus fecal shedding in children with inherited immune deficiencies.* J Infect Dis, 2012. **206**(8): p. 1269-74.
80. Roddie, C., et al., *Allogeneic hematopoietic stem cell transplantation and norovirus gastroenteritis: a previously unrecognized cause of morbidity.* Clin Infect Dis, 2009. **49**(7): p. 1061-8.
81. Schorn, R., et al., *Chronic norovirus infection after kidney transplantation: molecular evidence for immune-driven viral evolution.* Clin Infect Dis, 2010. **51**(3): p. 307-14.
82. Meeroff, J.C., et al., *Abnormal gastric motor function in viral gastroenteritis.* Ann Intern Med, 1980. **92**(3): p. 370-3.
83. Dolin, R., et al., *Viral gastroenteritis induced by the Hawaii agent. Jejunal histopathology and serologic response.* Am J Med, 1975. **59**(6): p. 761-8.
84. Schreiber, D.S., N.R. Blacklow, and J.S. Trier, *The mucosal lesion of the proximal small intestine in acute infectious nonbacterial gastroenteritis.* N Engl J Med, 1973. **288**(25): p. 1318-23.
85. Schreiber, D.S., N.R. Blacklow, and J.S. Trier, *The small intestinal lesion induced by Hawaii agent acute infectious nonbacterial gastroenteritis.* J Infect Dis, 1974. **129**(6): p. 705-8.
86. Troeger, H., et al., *Structural and functional changes of the duodenum in human norovirus infection.* Gut, 2009. **58**(8): p. 1070-7.
87. Karst, S.M., S. Zhu, and I.G. Goodfellow, *The molecular pathology of noroviruses.* J Pathol, 2015. **235**(2): p. 206-16.
88. Agus, S.G., et al., *Acute infectious nonbacterial gastroenteritis: intestinal histopathology. Histologic and enzymatic alterations during illness produced by the Norwalk agent in man.* Ann Intern Med, 1973. **79**(1): p. 18-25.
89. Chan, M.C., W.S. Ho, and J.J. Sung, *In vitro whole-virus binding of a norovirus genogroup II genotype 4 strain to cells of the lamina propria and Brunner's glands in the human duodenum.* J Virol, 2011. **85**(16): p. 8427-30.
90. Lay, M.K., et al., *Norwalk virus does not replicate in human macrophages or dendritic cells derived from the peripheral blood of susceptible humans.* Virology, 2010. **406**(1): p. 1-11.
91. Cheetham, S., et al., *Pathogenesis of a genogroup II human norovirus in gnotobiotic pigs.* J Virol, 2006. **80**(21): p. 10372-81.
92. Souza, M., et al., *Pathogenesis and immune responses in gnotobiotic calves after infection with the genogroup II.4-HS66 strain of human norovirus.* J Virol, 2008. **82**(4): p. 1777-86.
93. Mumphrey, S.M., et al., *Murine norovirus 1 infection is associated with histopathological changes in immunocompetent hosts, but clinical disease is prevented by STAT1-dependent interferon responses.* J Virol, 2007. **81**(7): p. 3251-63.

94. Parrino, T.A., et al., *Clinical immunity in acute gastroenteritis caused by Norwalk agent.* N Engl J Med, 1977. **297**(2): p. 86-9.
95. Johnson, P.C., et al., *Multiple-challenge study of host susceptibility to Norwalk gastroenteritis in US adults.* J Infect Dis, 1990. **161**(1): p. 18-21.
96. Malm, M., et al., *High serum levels of norovirus genotype-specific blocking antibodies correlate with protection from infection in children.* J Infect Dis, 2014. **210**(11): p. 1755-62.
97. Chadwick, P.R. and R. McCann, *Transmission of a small round structured virus by vomiting during a hospital outbreak of gastroenteritis.* J Hosp Infect, 1994. **26**(4): p. 251-9.
98. Teunis, P.F., et al., *Norwalk virus: how infectious is it?* J Med Virol, 2008. **80**(8): p. 1468-76.
99. Atmar, R.L., et al., *Norwalk virus shedding after experimental human infection.* Emerg Infect Dis, 2008. **14**(10): p. 1553-7.
100. Atmar, R.L., et al., *Determination of the 50% human infectious dose for Norwalk virus.* J Infect Dis, 2014. **209**(7): p. 1016-22.
101. Kirby, A.E., P.F. Teunis, and C.L. Moe, *Two human challenge studies confirm high infectivity of Norwalk virus.* J Infect Dis, 2015. **211**(1): p. 166-7.
102. Harris, J.P., B.A. Lopman, and S.J. O'Brien, *Infection control measures for norovirus: a systematic review of outbreaks in semi-enclosed settings.* J Hosp Infect, 2010. **74**(1): p. 1-9.
103. Buesa, J., et al., *Molecular epidemiology of caliciviruses causing outbreaks and sporadic cases of acute gastroenteritis in Spain.* J Clin Microbiol, 2002. **40**(8): p. 2854-9.
104. Haustein, T., et al., *Hospital admissions due to norovirus in adult and elderly patients in England.* Clin Infect Dis, 2009. **49**(12): p. 1890-2.
105. Mattison, K., *Norovirus as a foodborne disease hazard.* Adv Food Nutr Res, 2011. **62**: p. 1-39.
106. Friesema, I.H., et al., *Differences in clinical presentation between norovirus genotypes in nursing homes.* J Clin Virol, 2009. **46**(4): p. 341-4.
107. Simon, A., et al., *Norovirus outbreak in a pediatric oncology unit.* Scand J Gastroenterol, 2006. **41**(6): p. 693-9.
108. Holmes, J.D. and G.C. Simmons, *Gastrointestinal illness associated with a long-haul flight.* Epidemiol Infect, 2009. **137**(3): p. 441-7.
109. Kirking, H.L., et al., *Likely transmission of norovirus on an airplane, October 2008.* Clin Infect Dis, 2010. **50**(9): p. 1216-21.
110. Sala, M.R., et al., *An outbreak of food poisoning due to a genogroup I norovirus.* Epidemiol Infect, 2005. **133**(1): p. 187-91.
111. Zomer, T.P., et al., *A foodborne norovirus outbreak at a manufacturing company.* Epidemiol Infect, 2010. **138**(4): p. 501-6.
112. Godoy, P., et al., *[Outbreak of food-borne Norovirus associated with the consumption of sandwiches].* Med Clin (Barc), 2005. **124**(5): p. 161-4.
113. Gallay, A., et al., *A large multi-pathogen waterborne community outbreak linked to faecal contamination of a groundwater system, France, 2000.* Clin Microbiol Infect, 2006. **12**(6): p. 561-70.

114. Podewils, L.J., et al., *Outbreak of norovirus illness associated with a swimming pool.* Epidemiol Infect, 2007. **135**(5): p. 827-33.
115. Burkhardt, W., 3rd and K.R. Calci, *Selective accumulation may account for shellfish-associated viral illness.* Appl Environ Microbiol, 2000. **66**(4): p. 1375-8.
116. Ng, T.L., et al., *Oyster-associated outbreaks of Norovirus gastroenteritis in Singapore.* J Infect, 2005. **51**(5): p. 413-8.
117. Huppatz, C., et al., *A norovirus outbreak associated with consumption of NSW oysters: implications for quality assurance systems.* Commun Dis Intell Q Rep, 2008. **32**(1): p. 88-91.
118. David, S.T., et al., *An outbreak of norovirus caused by consumption of oysters from geographically dispersed harvest sites, British Columbia, Canada, 2004.* Foodborne Pathog Dis, 2007. **4**(3): p. 349-58.
119. Richards, G.P., *Enteric virus contamination of foods through industrial practices: a primer on intervention strategies.* J Ind Microbiol Biotechnol, 2001. **27**(2): p. 117-25.
120. Makary, P., et al., *Multiple norovirus outbreaks among workplace canteen users in Finland, July 2006.* Epidemiol Infect, 2009. **137**(3): p. 402-7.
121. Maunula, L., et al., *Detection of human norovirus from frozen raspberries in a cluster of gastroenteritis outbreaks.* Euro Surveill, 2009. **14**(49).
122. Wadl, M., et al., *Food-borne norovirus-outbreak at a military base, Germany, 2009.* BMC Infect Dis, 2010. **10**: p. 30.
123. Gallimore, C.I., et al., *Detection of multiple enteric virus strains within a foodborne outbreak of gastroenteritis: an indication of the source of contamination.* Epidemiol Infect, 2005. **133**(1): p. 41-7.
124. Ethelberg, S., et al., *Outbreaks of gastroenteritis linked to lettuce, Denmark, January 2010.* Euro Surveill, 2010. **15**(6).
125. Seo, K., et al., *Effect of temperature, pH, and NaCl on the inactivation kinetics of murine norovirus.* J Food Prot, 2012. **75**(3): p. 533-40.
126. Bozkurt, H., D.H. D'Souza, and P.M. Davidson, *Determination of the thermal inactivation kinetics of the human norovirus surrogates, murine norovirus and feline calicivirus.* J Food Prot, 2013. **76**(1): p. 79-84.
127. Lee, J., K. Zoh, and G. Ko, *Inactivation and UV disinfection of murine norovirus with TiO2 under various environmental conditions.* Appl Environ Microbiol, 2008. **74**(7): p. 2111-7.
128. Feng, K., et al., *Inactivation of a human norovirus surrogate, human norovirus virus-like particles, and vesicular stomatitis virus by gamma irradiation.* Appl Environ Microbiol, 2011. **77**(10): p. 3507-17.
129. Shirasaki, N., et al., *Estimation of norovirus removal performance in a coagulation-rapid sand filtration process by using recombinant norovirus VLPs.* Water Res, 2010. **44**(5): p. 1307-16.
130. Lou, F., et al., *Inactivation of a human norovirus surrogate by high-pressure processing: effectiveness, mechanism, and potential application in the fresh produce industry.* Appl Environ Microbiol, 2011. **77**(5): p. 1862-71.
131. Park, G.W., et al., *Comparative efficacy of seven hand sanitizers against murine norovirus, feline calicivirus, and GII.4 norovirus.* J Food Prot, 2010. **73**(12): p. 2232-8.

132. Liu, P., et al., *Immunomagnetic separation combined with RT-qPCR for determining the efficacy of disinfectants against human noroviruses.* J Infect Public Health, 2015. **8**(2): p. 145-54.
133. Takimoto, K., et al., *Effect of hypochlorite-based disinfectants on inactivation of murine norovirus and attempt to eliminate or prevent infection in mice by addition to drinking water.* Exp Anim, 2013. **62**(3): p. 237-45.
134. Bentley, K., et al., *Hydrogen peroxide vapour decontamination of surfaces artificially contaminated with norovirus surrogate feline calicivirus.* J Hosp Infect, 2012. **80**(2): p. 116-21.
135. Lim, M.Y., et al., *Characterization of ozone disinfection of murine norovirus.* Appl Environ Microbiol, 2010. **76**(4): p. 1120-4.
136. Magulski, T., et al., *Inactivation of murine norovirus by chemical biocides on stainless steel.* BMC Infect Dis, 2009. **9**: p. 107.
137. Jimenez, L. and M. Chiang, *Virucidal activity of a quaternary ammonium compound disinfectant against feline calicivirus: a surrogate for norovirus.* Am J Infect Control, 2006. **34**(5): p. 269-73.
138. Liu, P., et al., *Effectiveness of liquid soap and hand sanitizer against Norwalk virus on contaminated hands.* Appl Environ Microbiol, 2010. **76**(2): p. 394-9.
139. Lindesmith, L., et al., *Human susceptibility and resistance to Norwalk virus infection.* Nat Med, 2003. **9**(5): p. 548-53.
140. Neyens, E., et al., *Advanced sludge treatment affects extracellular polymeric substances to improve activated sludge dewatering.* J Hazard Mater, 2004. **106**(2-3): p. 83-92.
141. Hennessy, E.P., et al., *Norwalk virus infection and disease is associated with ABO histo-blood group type.* J Infect Dis, 2003. **188**(1): p. 176-7.
142. Bartsch, S.M., et al., *The potential economic value of a human norovirus vaccine for the United States.* Vaccine, 2012. **30**(49): p. 7097-104.
143. Hale, A.D., et al., *Expression and self-assembly of Grimsby virus: antigenic distinction from Norwalk and Mexico viruses.* Clin Diagn Lab Immunol, 1999. **6**(1): p. 142-5.
144. El-Kamary, S.S., et al., *Adjuvanted intranasal Norwalk virus-like particle vaccine elicits antibodies and antibody-secreting cells that express homing receptors for mucosal and peripheral lymphoid tissues.* J Infect Dis, 2010. **202**(11): p. 1649-58.
145. Bernstein, D.I., et al., *Norovirus Vaccine Against Experimental Human GII.4 Virus Illness: A Challenge Study in Healthy Adults.* J Infect Dis, 2015. **211**(6): p. 870-8.
146. Papafragkou, E., et al., *Challenges of culturing human norovirus in three-dimensional organoid intestinal cell culture models.* PLoS One, 2014. **8**(6): p. e63485.
147. Miura, T., et al., *Histo-blood group antigen-like substances of human enteric bacteria as specific adsorbents for human noroviruses.* J Virol, 2013. **87**(17): p. 9441-51.
148. Taube, S., et al., *A mouse model for human norovirus.* MBio, 2013. **4**(4).
149. Wyatt, R.G., et al., *Experimental infection of chimpanzees with the Norwalk agent of epidemic viral gastroenteritis.* J Med Virol, 1978. **2**(2): p. 89-96.
150. Rockx, B.H., et al., *Experimental norovirus infections in non-human primates.* J Med Virol, 2005. **75**(2): p. 313-20.
151. Karst, S.M., et al., *STAT1-dependent innate immunity to a Norwalk-like virus.* Science, 2003. **299**(5612): p. 1575-8.

152. Shortland, A., et al., *Pathology caused by persistent murine norovirus infection.* J Gen Virol, 2014. **95**(Pt 2): p. 413-22.
153. Yunus, M.A., et al., *The murine norovirus core subgenomic RNA promoter consists of a stable stem-loop that can direct accurate initiation of RNA synthesis.* J Virol, 2015. **89**(2): p. 1218-29.
154. Davies, C., et al., *Murine Norovirus replication induces a G0/G1 cell cycle arrest in asynchronous growing cells.* J Virol, 2015.
155. Farkas, T., et al., *Characterization of a rhesus monkey calicivirus representing a new genus of Caliciviridae.* J Virol, 2008. **82**(11): p. 5408-16.
156. Sestak, K., et al., *Experimental inoculation of juvenile rhesus macaques with primate enteric caliciviruses.* PLoS One, 2012. **7**(5): p. e37973.
157. Zhang, D., et al., *Tulane virus recognizes the A type 3 and B histo-blood group antigens.* J Virol, 2015. **89**(2): p. 1419-27.
158. Hirneisen, K.A. and K.E. Kniel, *Comparing human norovirus surrogates: murine norovirus and Tulane virus.* J Food Prot, 2013. **76**(1): p. 139-43.
159. Goodfellow, I.G., *Calicivirus Reverse Genetics*, in *Reverse Genetics of RNA Viruses: Applications and Perspectives*, A. Bridgen, Editor. 2013, John Wiley & Sons Ltd. p. 82-98.
160. Sosnovstev, S., S. Sosnovtseva, and K.Y. Green., *Recovery of feline calicivirus from plasmid DNA containing a full-length copy of the genome*, in *The 1st International Symposium on Caliciviruses*, R.M.G. D. Chasey, I.N. Clarke, Editor. 1996, European Society for Veterinary Virology and Central Veterinary Laboratory: Reading, United Kingdom. p. 125-130.
161. Chang, K.O., et al., *Reverse genetics system for porcine enteric calicivirus, a prototype sapovirus in the Caliciviridae.* J Virol, 2005. **79**(3): p. 1409-16.
162. Chaudhry, Y., M.A. Skinner, and I.G. Goodfellow, *Recovery of genetically defined murine norovirus in tissue culture by using a fowlpox virus expressing T7 RNA polymerase.* J Gen Virol, 2007. **88**(Pt 8): p. 2091-100.
163. Liu, G., et al., *A DNA-launched reverse genetics system for rabbit hemorrhagic disease virus reveals that the VP2 protein is not essential for virus infectivity.* J Gen Virol, 2008. **89**(Pt 12): p. 3080-5.
164. Wei, C., et al., *Recovery of infectious virus by transfection of in vitro-generated RNA from tulane calicivirus cDNA.* J Virol, 2008. **82**(22): p. 11429-36.
165. Sandoval-Jaime, C., K.Y. Green, and S.V. Sosnovtsev, *Recovery of murine norovirus and feline calicivirus from plasmids encoding EMCV IRES in stable cell lines expressing T7 polymerase.* J Virol Methods, 2015. **217**: p. 1-7.
166. Katayama, K., et al., *Investigation of norovirus replication in a human cell line.* Arch Virol, 2006. **151**(7): p. 1291-308.
167. Katayama, K., et al., *Plasmid-based human norovirus reverse genetics system produces reporter-tagged progeny virus containing infectious genomic RNA.* Proc Natl Acad Sci U S A, 2014. **111**(38): p. E4043-52.
168. Bull, R.A. and P.A. White, *Mechanisms of GII.4 norovirus evolution.* Trends Microbiol, 2011. **19**(5): p. 233-40.
169. Hotard, A.L., et al., *A stabilized respiratory syncytial virus reverse genetics system amenable to recombination-mediated mutagenesis.* Virology, 2012. **434**(1): p. 129-36.

170. Kwilas, A.R., et al., *Respiratory syncytial virus engineered to express the cystic fibrosis transmembrane conductance regulator corrects the bioelectric phenotype of human cystic fibrosis airway epithelium in vitro.* J Virol, 2010. **84**(15): p. 7770-81.
171. Walker, S.C., J.M. Avis, and G.L. Conn, *General plasmids for producing RNA in vitro transcripts with homogeneous ends.* Nucleic Acids Res, 2003. **31**(15): p. e82.
172. Coleman, J.R., et al., *Virus attenuation by genome-scale changes in codon pair bias.* Science, 2008. **320**(5884): p. 1784-7.
173. Vega, E., et al., *RNA populations in immunocompromised patients as reservoirs for novel norovirus variants.* J Virol, 2014. **88**(24): p. 14184-96.
174. Studier, F.W., et al., *Use of T7 RNA polymerase to direct expression of cloned genes.* Methods Enzymol, 1990. **185**: p. 60-89.
175. Kageyama, T., et al., *Broadly reactive and highly sensitive assay for Norwalk-like viruses based on real-time quantitative reverse transcription-PCR.* J Clin Microbiol, 2003. **41**(4): p. 1548-57.